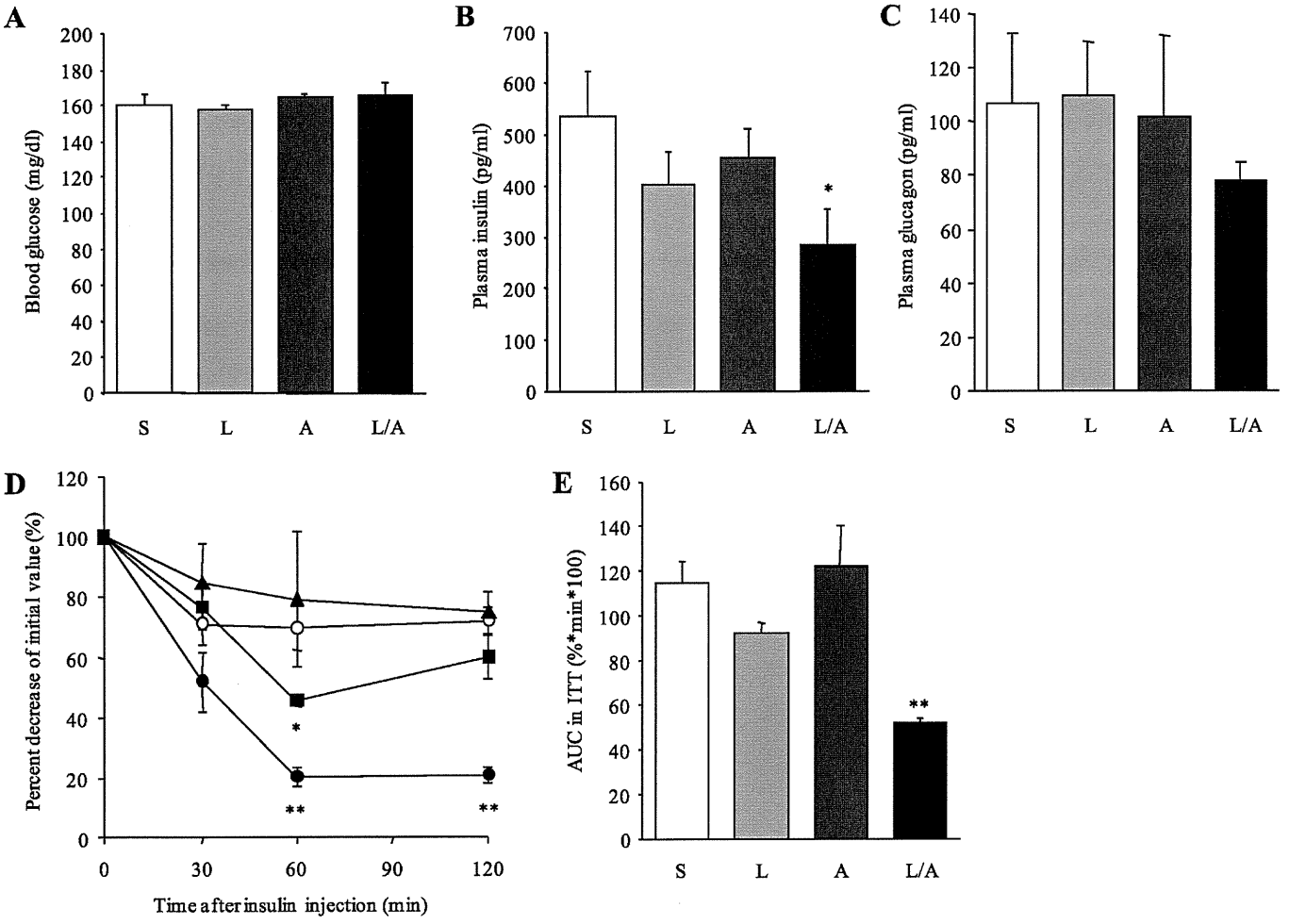

Fig. 2. Effect of L and/or A on glucose metabolism in DIO mice. Blood glucose (*A*), plasma insulin (*B*), and plasma glucagon levels (*C*) under ad libitum feeding on *day 14* in S, L, A, and L/A-treated mice. Values are means ± SE (n = 8–9/group). %Change of initial value of blood glucose levels (*D*) and area under the curve (AUC; *E*) during the insulin tolerance test (ITT) on *day 10* in S (○), L (■), A (▲), and L/A-treated mice (●). Values are means ± SE (n = 4/group). *P < 0.05 and **P < 0.01 vs. S-treated mice.

contents. Liver weight was significantly decreased (by 16%) in L/A-treated mice compared with that in S-treated mice (Fig. 3*A*). In addition, L/A coadministration significantly decreased triglyceride contents in liver (by 42%) and skeletal muscle (by 46%), whereas administration of L or A alone did not decrease tissue triglyceride contents compared with saline administration (Fig. 3, *B* and *C*).

Leptin has been shown to decrease skeletal muscle triglyceride content in part by increasing fatty acid β-oxidation through AMPKα2 activation in skeletal muscle (24). Therefore, we measured AMPK activity in soleus muscle, where the effect of leptin on AMPK activation was pronounced (24). AMPKα1 activity in soleus muscle was not changed significantly in any group of mice compared with S-treated mice (Fig. 3*D*). On the other hand, AMPKα2 activity in soleus muscle was increased significantly only in L/A-treated mice (by 71%) compared with those in S-treated mice (Fig. 3*E*), consistent with the results of tissue triglyceride contents.

Pair-feeding and weight-matched calorie restriction experiments. We performed pair-feeding experiments to assess whether the body weight reduction and the enhancement of insulin sensitivity by L/A coadministration was associated with food intake reduction. Pair-feeding to L/A-treated mice reduced body weight in DIO mice significantly, but the change was apparently smaller than in L/A-treated mice (Fig. 4*A*). In addition, PF mice showed neither the improvement in insulin sensitivity (Fig. 4, *B* and *C*) nor the decrease in triglyceride contents of liver and skeletal muscle (Fig. 4, *D* and *E*), in contrast to L/A-treated mice.

Then, we performed weight-matched calorie restriction experiments to assess whether the enhancement of insulin sensitivity by L/A coadministration was associated with body weight reduction. To match the body weight to L/A-treated mice, the food intake was restricted to 70% of S-treated mice in CR mice (Fig. 4*A*). In this condition, CR mice showed neither the improvement of insulin sensitivity (Fig. 4, *B* and *C*) nor the decrease in triglyceride contents of liver and skeletal muscle (Fig. 4, *D* and *E*), in contrast to L/A-treated mice.

DISCUSSION

Leptin could be an ideal drug for obesity-associated diabetes because it has both a weight-reducing effect and an antidiabetic effect. However, even high pharmacological doses of leptin elicit only marginal weight loss in non-leptin-deficient DIO rodents and humans (8, 15), whereas leptin replacement ther-

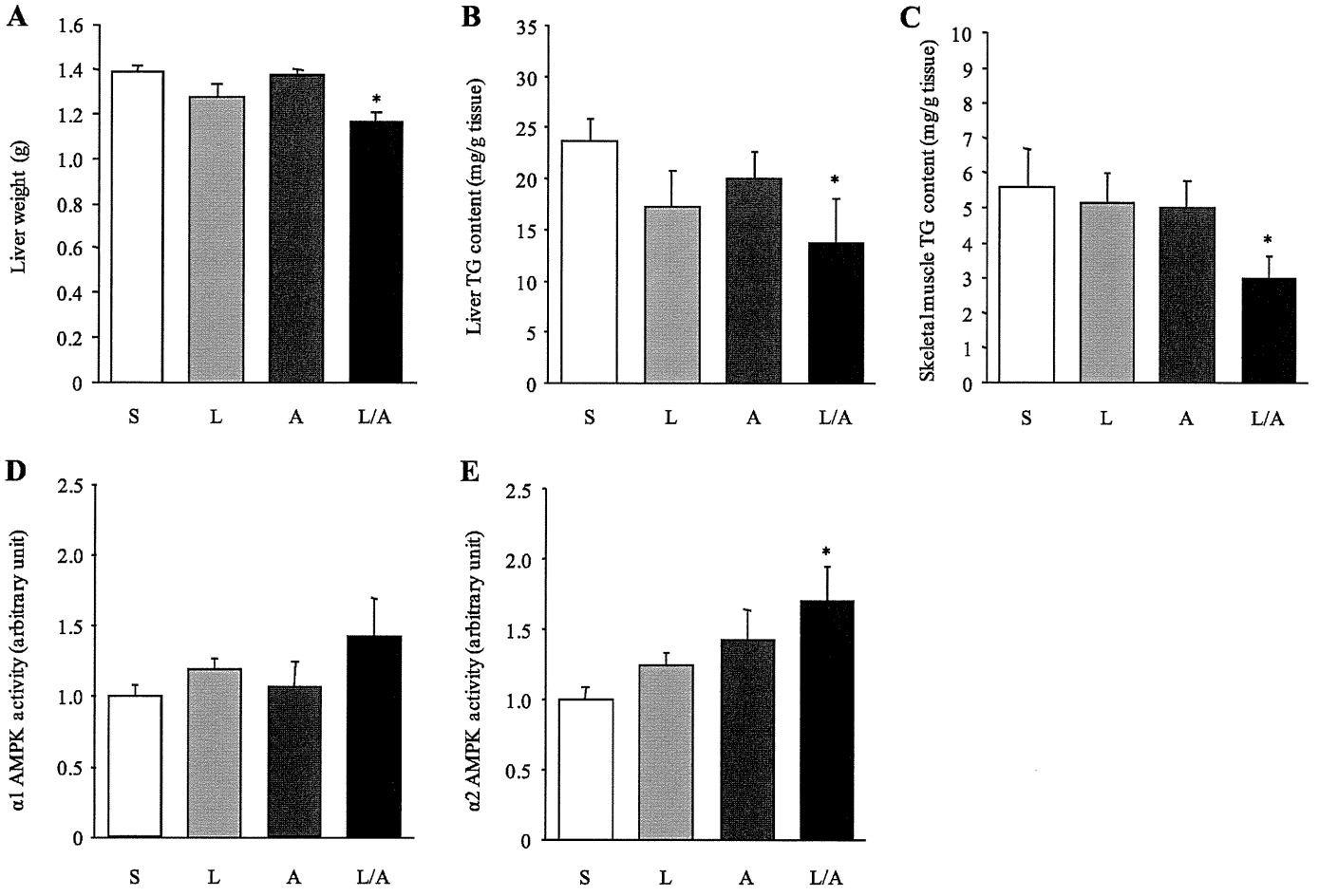

Fig. 3. Effect of L and/or A on tissue triglyceride (TG) content and skeletal muscle AMP-activated protein kinase (AMPK) activity in DIO mice. Liver size (*A*) and liver (*B*) and gastrocnemius muscle (*C*) TG contents on *day 14* in S, L, A, and L/A-treated mice. AMPKα1 (*D*) and AMPKα2 activity (*E*) on *day 14* in soleus muscle of S, L, A, and L/A-treated mice. Values are means ± SE (n = 8–9/group). *$P < 0.05$ vs. S-treated mice.

apy induces profound weight loss in leptin-deficient mice and humans (10, 13). The obese state is thus thought to be associated with leptin resistance, wherein overweight/obese individuals become insensitive to high circulating leptin levels. Sensitizing agents of leptin's effects are expected to treat obesity-associated diabetes comprehensively. In this study, we demonstrated that L/A coadministration not only reduced food intake and body weight but also enhanced insulin sensitivity accompanied by an increase of AMPKα2 activity in skeletal muscle and decrease of tissue triglyceride contents in leptin-resistant DIO mice. Our results indicate the possible clinical usefulness of L/A coadministration as a new antidiabetic treatment in obesity-associated diabetes.

Recently, coadministration of L (500 $\mu g \cdot kg^{-1} \cdot day^{-1}$) and A (100 $\mu g \cdot kg^{-1} \cdot day^{-1}$) was shown to result in a synergistic fat-specific body weight reduction in DIO rats (34). The synergistic antiobesity effect of leptin and amylin was established by the response surface methodology analysis using lower dose ranges of L (0–125 $\mu g \cdot kg^{-1} \cdot day^{-1}$) and A (0–50 $\mu g \cdot kg^{-1} \cdot day^{-1}$) in DIO rats (39). However, because the study of L/A coadministration was not fully examined in mice, the adequate doses of L and A were unclear in DIO mice. Therefore, we chose L (500 $\mu g \cdot kg^{-1} \cdot day^{-1}$) and A (100 $\mu g \cdot kg^{-1} \cdot day^{-1}$) in the present study according to the first report (34). Administration of L (500 $\mu g \cdot g^{-1} \cdot day^{-1}$) had no significant effect on food intake or body weight in DIO mice (Fig. 1, *A* and *B*). Although amylin itself has been shown to dose-dependently reduce food intake and body weight (20, 26), administration of A (100 $\mu g \cdot kg^{-1} \cdot day^{-1}$) was not effective in our DIO mice (Fig. 1, *A* and *B*). Under these conditions, L/A coadministration reduced food intake and body weight in DIO mice in a greater than mathematically additive manner (Fig. 1, *A* and *B*). Our data support that L/A coadministration is a useful treatment for obesity beyond species difference. With the dose of leptin used in the present study, the plasma leptin level in DIO mice increased to 45.1–53.0 ng/ml (Table 2), which can be seen in human obese subjects. In addition, higher leptin levels were obtained in the obese human clinical trial without any clinically significant adverse effects on major organ systems (15). Therefore, the leptin level achieved with the dose used in the present study could be clinically applied in humans.

In general, amylin is considered not to affect insulin secretion and insulin sensitivity but rather to complement the effects of insulin on circulating glucose levels through two main mechanisms (43). First, amylin suppresses postprandial glucagon secretion, thereby decreasing glucagon-stimulated hepatic glucose output following nutrient ingestion (12). Second, amylin also slows the rate of gastric emptying and thus the rate at which nutrients are delivered from the stomach to the small intestine for absorption (44, 45). On the other hand, leptin is

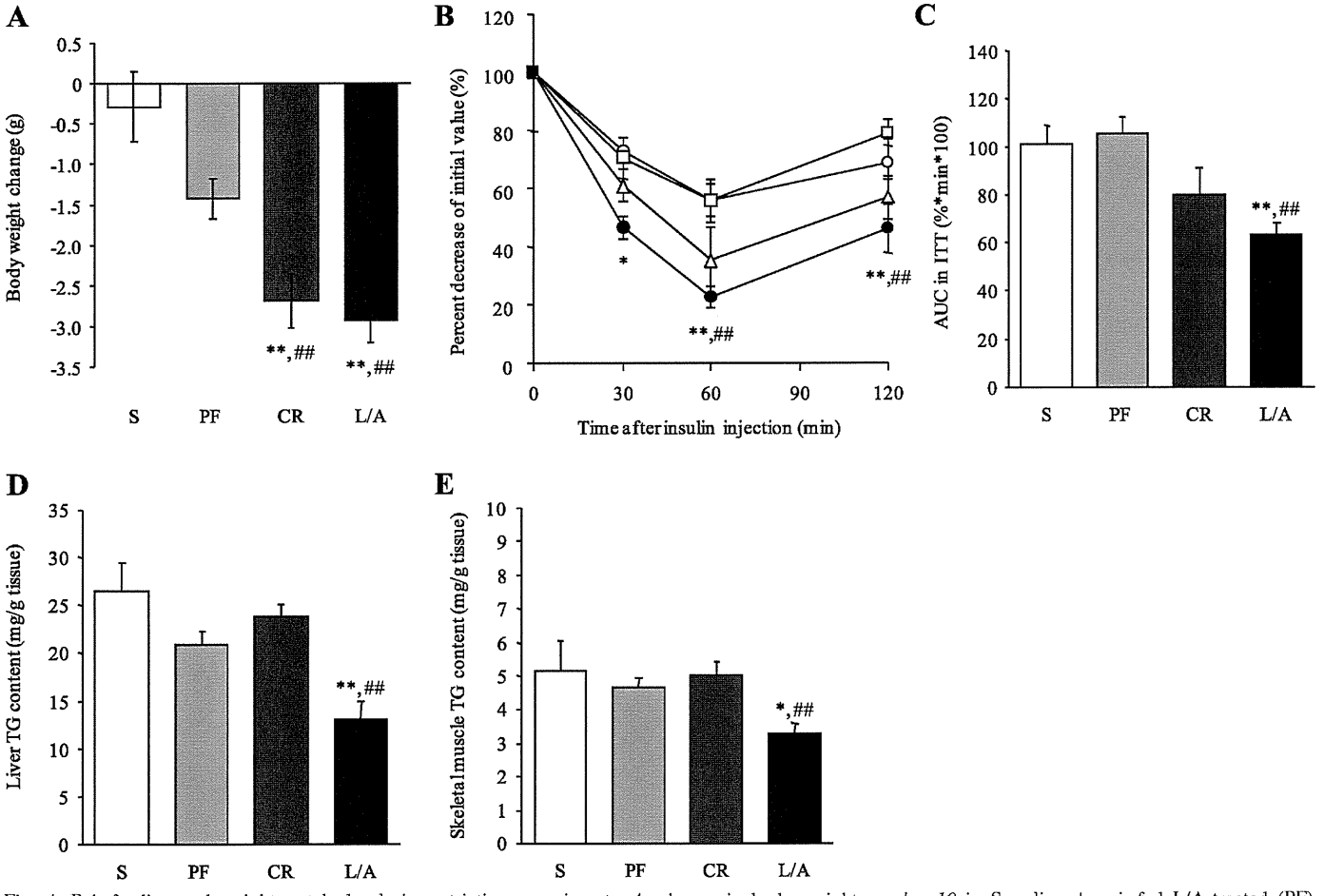

Fig. 4. Pair-feeding and weight-matched calorie restriction experiments. *A*: change in body weight on *day 10* in S, saline + pair-fed L/A-treated (PF), weight-matched DIO (CR), and L/A-treated mice. %Decrease of initial value of blood glucose levels (*B*) and AUC (*C*) during the ITT on *day 10* in S (○), PF (□), CR (△), and L/A-treated mice (●). Liver (*D*) and gastrocnemius muscle (*E*) TG contents on *day 14* in S, PF, CR, and L/A-treated mice. Values are means ± SE (n = 7–12/group). *$P < 0.05$ and **$P < 0.01$ vs. S-treated mice; ##$P < 0.01$ vs. PF mice.

considered to increase insulin sensitivity with augmentation of insulin receptor signaling in insulin target organs such as the liver and skeletal muscle (30) and suppress secretion of glucagon (28, 42). In this study, the tendency toward a decrease, but not a significant one, in plasma glucagon levels was observed in L/A-treated mice (Fig. 2*C*). Further studies are needed to evaluate the effect of leptin on plasma glucagon in DIO mice. Administration of L or A alone did not affect insulin sensitivity in DIO mice (Fig. 2, *A–D*). However, L/A coadministration effectively enhanced insulin sensitivity in DIO mice (Fig. 2, *A–D*). Taken together, our results indicate that amylin improved the insulin-sensitizing action of leptin in DIO mice.

One of the mechanisms by which leptin enhances insulin sensitivity is the reduction of fat accumulation in insulin target organs by activation of the AMPKα2 in skeletal muscle (24, 37, 38). In this study, we demonstrated that only L/A coadministration significantly reduced liver and skeletal muscle triglyceride contents accompanied by AMPKα2 activation in the skeletal muscle (Fig. 3, *A–E*). Previously, we demonstrated that AMPK in skeletal muscle was activated and insulin sensitivity enhanced in LepTg mice. High-fat diet feeding diminished both the activation of AMPK and the enhancement of insulin sensitivity, and diet substitution to standard diet restored them in LepTg mice, indicating that AMPK activity in skeletal muscle closely parallels insulin sensitivity (37). Based on the results of LepTg mice, we proposed that the AMPK activity in peripheral tissues could be a novel biochemical marker of leptin sensitivity in vivo (37). Therefore, the increase of AMPK activity in L/A-treated mice suggests that amylin improved leptin sensitivity in leptin-resistant DIO mice.

For the treatment of obesity-associated diabetes, it is universally accepted that dietary management is used initially with specific emphasis on weight reduction, because weight reduction leads to improvement in deteriorated glucose metabolism (1, 3). Therefore, to assess the influence of food intake and body weight reduction, we compared insulin sensitivity and tissue triglyceride contents among PF, CR, and L/A-treated mice. In this study, PF mice did not show reduced body weight compared with L/A-treated mice (Fig. 4*A*). Because amylin-induced weight loss was attributable primarily to reduced food intake (20, 33, 35), weight loss in L/A-treated mice suggests additional mechanisms such as restoration of leptin's effect on energy expenditure. In previous analyses of calorie restriction effects on metabolism, calorie restriction was accompanied by an expected counterregulatory decline in energy expenditure in rodents (39). However, in this study, we showed that L/A coadministration increased energy expenditure significantly,

whereas it reduced food intake (Fig. 1*C*). In addition, CR mice, whose food consumption was restricted to match their body weight to those of the L/A-treated mice, showed neither the improvement of insulin sensitivity (Fig. 4, *B* and *C*) nor the decrease in liver and skeletal muscle triglyceride contents (Fig. 4, *D* and *E*). These results showed that the improvement of insulin sensitivity and the decrease in tissue triglyceride contents by L/A coadministration were achieved by other mechanisms besides calorie restriction.

In conclusion, we demonstrated that L/A coadministration effectively improves insulin sensitivity in addition to reducing food intake and body weight in DIO mice. Our data indicate that L/A coadministration could be a new antidiabetic treatment in obesity-associated diabetes.

ACKNOWLEDGMENTS

We thank Mayumi Nagamoto, Kyoto University Graduate School of Medicine, for technical assistance and Yoko Koyama, Kyoto University Graduate School of Medicine, for secretarial assistance.

GRANTS

This work was supported in part by research grants from the Ministry of Education, Culture, Sports, Science, and Technology of Japan, the Ministry of Health, Labor, and Welfare of Japan, the Japan Foundation for Applied Enzymology, and the Fujiwara Memorial Foundation.

DISCLOSURES

No conflicts of interest, financial or otherwise, are declared by the authors.

AUTHOR CONTRIBUTIONS

T.K., K.E., and K.N. did the conception and design of the research; T.K., T.S., and L.M. performed the experiments; T.K., T.S., and L.M. analyzed the data; T.K., K.E., T.S., L.M., D.A., Y.Y., S.Y.-K., M.A.-A., J.F., K.H., and K.N. interpreted the results of the experiments; T.K. prepared the figures; T.K. drafted the manuscript; T.K. and K.E. edited and revised the manuscript; T.K., K.E., and K.N. approved the final version of the manuscript.

REFERENCES

1. **Amatruda JM, Richeson JF, Welle SL, Brodows RG, Lockwood DH.** The safety and efficacy of a controlled low-energy ("very-low-calorie") diet in the treatment of non-insulin-dependent diabetes and obesity. *Arch Intern Med* 148: 873–877, 1988.
2. **Beltrand J, Beregszaszi M, Chevenne D, Sebag G, De Kerdanet M, Huet F, Polak M, Tubiana-Rufi N, Lacombe D, De Paoli AM, Levy-Marchal C.** Metabolic correction induced by leptin replacement treatment in young children with Berardinelli-Seip congenital lipoatrophy. *Pediatrics* 120: e291–e296, 2007.
3. **Campfield LA, Smith FJ, Burn P.** Strategies and potential molecular targets for obesity treatment. *Science* 280: 1383–1387, 1998.
4. **Cooper GJ, Leighton B, Dimitriadis GD, Parry-Billings M, Kowalchuk JM, Howland K, Rothbard JB, Willis AC, Reid KB.** Amylin found in amyloid deposits in human type 2 diabetes mellitus may be a hormone that regulates glycogen metabolism in skeletal muscle. *Proc Natl Acad Sci USA* 85: 7763–7766, 1988.
5. **Ebihara K, Kusakabe T, Hirata M, Masuzaki H, Miyanaga F, Kobayashi N, Tanaka T, Chusho H, Miyazawa T, Hayashi T, Hosoda K, Ogawa Y, DePaoli AM, Fukushima M, Nakao K.** Efficacy and safety of leptin-replacement therapy and possible mechanisms of leptin actions in patients with generalized lipodystrophy. *J Clin Endocrinol Metab* 92: 532–541, 2007.
6. **Ebihara K, Masuzaki H, Nakao K.** Long-term leptin-replacement therapy for lipoatrophic diabetes. *N Engl J Med* 351: 615–616, 2004.
7. **Ebihara K, Ogawa Y, Masuzaki H, Shintani M, Miyanaga F, Aizawa-Abe M, Hayashi T, Hosoda K, Inoue G, Yoshimasa Y, Gavrilova O, Reitman ML, Nakao K.** Transgenic overexpression of leptin rescues insulin resistance and diabetes in a mouse model of lipoatrophic diabetes. *Diabetes* 50: 1440–1448, 2001.
8. **El-Haschimi K, Pierroz DD, Hileman SM, Bjørbaek C, Flier JS.** Two defects contribute to hypothalamic leptin resistance in mice with diet-induced obesity. *J Clin Invest* 105: 1827–1832, 2000.
9. **Elmquist JK, Elias CF, Saper CB.** From lesions to leptin: hypothalamic control of food intake and body weight. *Neuron* 22: 221–232, 1999.
10. **Farooqi IS, Jebb SA, Langmack G, Lawrence E, Cheetham CH, Prentice AM, Hughes IA, McCamish MA, O'Rahilly S.** Effects of recombinant leptin therapy in a child with congenital leptin deficiency. *N Engl J Med* 341: 879–884, 1999.
11. **Friedman JM, Halaas JL.** Leptin and the regulation of body weight in mammals. *Nature* 395: 763–770, 1998.
12. **Gedulin BR, Rink TJ, Young AA.** Dose-response for glucagonostatic effect of amylin in rats. *Metabolism* 46: 67–70, 1997.
13. **Halaas JL, Gajiwala KS, Maffei M, Cohen SL, Chait BT, Rabinowitz D, Lallone RL, Burley SK, Friedman JM.** Weight-reducing effects of the plasma protein encoded by the obese gene. *Science* 269: 543–546, 1995.
14. **Hedbacker K, Birsoy K, Wysocki RW, Asilmaz E, Ahima RS, Farooqi IS, Friedman JM.** Antidiabetic effects of IGFBP2, a leptin-regulated gene. *Cell Metab* 11: 11–22, 2010.
15. **Heymsfield SB, Greenberg AS, Fujioka K, Dixon RM, Kushner R, Hunt T, Lubina JA, Patane J, Self B, Hunt P, McCamish M.** Recombinant leptin for weight loss in obese and lean adults: a randomized, controlled, dose-escalation trial. *JAMA* 282: 1568–1575, 1999.
16. **Hosoda K, Masuzaki H, Ogawa Y, Miyawaki T, Hiraoka J, Hanaoka I, Yasuno A, Nomura T, Fujisawa Y, Yoshimasa Y, Nishi S, Yamori Y, Nakao K.** Development of radioimmunoassay for human leptin. *Biochem Biophys Res Commun* 221: 234–239, 1996.
17. **Kamohara S, Burcelin R, Halaas JL, Friedman JM, Charron MJ.** Acute stimulation of glucose metabolism in mice by leptin treatment. *Nature* 389: 374–377, 1997.
18. **Kusakabe T, Tanioka H, Ebihara K, Hirata M, Miyamoto L, Miyanaga F, Hige H, Aotani D, Fujisawa T, Masuzaki H, Hosoda K, Nakao K.** Beneficial effects of leptin on glycaemic and lipid control in a mouse model of type 2 diabetes with increased adiposity induced by streptozotocin and a high-fat diet. *Diabetologia* 52: 675–683, 2009.
19. **Lutz TA.** Amylinergic control of food intake. *Physiol Behav* 89: 465–471, 2006.
20. **Lutz TA, Del Prete E, Scharrer E.** Reduction of food intake in rats by intraperitoneal injection of low doses of amylin. *Physiol Behav* 55: 891–895, 1994.
21. **Lutz TA, Mollet A, Rushing PA, Riediger T, Scharrer E.** The anorectic effect of a chronic peripheral infusion of amylin is abolished in area postrema/nucleus of the solitary tract (AP/NTS) lesioned rats. *Int J Obes Relat Metab Disord* 25: 1005–1011, 2001.
22. **Lutz TA, Senn M, Althaus J, Del Prete E, Ehrensperger F, Scharrer E.** Lesion of the area postrema/nucleus of the solitary tract (AP/NTS) attenuates the anorectic effects of amylin and calcitonin gene-related peptide (CGRP) in rats. *Peptides* 19: 309–317, 1998.
23. **Maffei M, Halaas J, Ravussin E, Pratley RE, Lee GH, Zhang Y, Fei H, Kim S, Lallone R, Ranganathan S, Kern PA, Friedman JM.** Leptin levels in human and rodent: measurement of plasma leptin and ob RNA in obese and weight-reduced subjects. *Nat Med* 1: 1155–1161, 1995.
24. **Minokoshi Y, Kim YB, Peroni OD, Fryer LG, Müller C, Carling D, Kahn BB.** Leptin stimulates fatty-acid oxidation by activating AMP-activated protein kinase. *Nature* 415: 339–343, 2002.
25. **Miyanaga F, Ogawa Y, Ebihara K, Hidaka S, Tanaka T, Hayashi S, Masuzaki H, Nakao K.** Leptin as an adjunct of insulin therapy in insulin-deficient diabetes. *Diabetologia* 46: 1329–1337, 2003.
26. **Morley JE, Flood JF, Horowitz M, Morley PM, Walter MJ.** Modulation of food intake by peripherally administered amylin. *Am J Physiol Regul Integr Comp Physiol* 267: R178–R184, 1994.
27. **Myers MG Jr, Münzberg H, Leinninger GM, Leshan RL.** The geometry of leptin action in the brain: more complicated than a simple ARC. *Cell Metab* 9: 117–123, 2009.
28. **Naito M, Fujikura J, Ebihara K, Miyanaga F, Yokoi H, Kusakabe T, Yamamoto Y, Son C, Mukoyama M, Hosoda K, Nakao K.** Therapeutic impact of leptin on diabetes, diabetic complications, and longevity in insulin-deficient diabetic mice. *Diabetes* 60: 2265–2273, 2011.
29. **Nakao K, Yasoda A, Ebihara K, Hosoda K, Mukoyama M.** Translational research of novel hormones: lessons from animal models and rare human diseases for common human diseases. *J Mol Med* 87: 1029–1039, 2009.

30. **Ogawa Y, Masuzaki H, Hosoda K, Aizawa-Abe M, Suga J, Suda M, Ebihara K, Iwai H, Matsuoka N, Satoh N, Odaka H, Kasuga H, Fujisawa Y, Inoue G, Nishimura H, Yoshimasa Y, Nakao K.** Increased glucose metabolism and insulin sensitivity in transgenic skinny mice overexpressing leptin. *Diabetes* 48: 1822–1829, 1999.
31. **Oral EA, Simha V, Ruiz E, Andewelt A, Premkumar A, Snell P, Wagner AJ, DePaoli AM, Reitman ML, Taylor SI, Gorden P, Garg A.** Leptin-replacement therapy for lipodystrophy. *N Engl J Med* 346: 570–578, 2002.
32. **Ravussin E, Smith SR, Mitchell JA, Shringarpure R, Shan K, Maier H, Koda JE, Weyer C.** Enhanced weight loss with pramlintide/metreleptin: an integrated neurohormonal approach to obesity pharmacotherapy. *Obesity (Silver Spring)* 17: 1736–1743, 2009.
33. **Roth JD, Hughes H, Kendall E, Baron AD, Anderson CM.** Antiobesity effects of the beta-cell hormone amylin in diet-induced obese rats: effects on food intake, body weight, composition, energy expenditure, and gene expression. *Endocrinology* 147: 5855–5864, 2006.
34. **Roth JD, Roland BL, Cole RL, Trevaskis JL, Weyer C, Koda JE, Anderson CM, Parkes DG, Baron AD.** Leptin responsiveness restored by amylin agonism in diet-induced obesity: evidence from nonclinical and clinical studies. *Proc Natl Acad Sci USA* 105: 7257–7262, 2008.
35. **Rushing PA, Hagan MM, Seeley RJ, Lutz TA, Woods SC.** Amylin: a novel action in the brain to reduce body weight. *Endocrinology* 141: 850–853, 2000.
36. **Shulman GI.** Cellular mechanisms of insulin resistance. *J Clin Invest* 106: 171–176, 2000.
37. **Tanaka T, Hidaka S, Masuzaki H, Yasue S, Minokoshi Y, Ebihara K, Chusho H, Ogawa Y, Toyoda T, Sato K, Miyanaga F, Fujimoto M, Tomita T, Kusakabe T, Kobayashi N, Tanioka H, Hayashi T, Hosoda K, Yoshimatsu H, Sakata T, Nakao K.** Skeletal muscle AMP-activated protein kinase phosphorylation parallels metabolic phenotype in leptin transgenic mice under dietary modification. *Diabetes* 54: 2365–2374, 2005.
38. **Tanaka T, Masuzaki H, Yasue S, Ebihara K, Shiuchi T, Ishii T, Arai N, Hirata M, Yamamoto H, Hayashi T, Hosoda K, Minokoshi Y, Nakao K.** Central melanocortin signaling restores skeletal muscle AMP-activated protein kinase phosphorylation in mice fed a high-fat diet. *Cell Metab* 5: 395–402, 2007.
39. **Trevaskis JL, Coffey T, Cole R, Lei C, Wittmer C, Walsh B, Weyer C, Koda J, Baron AD, Parkes DG, Roth JD.** Amylin-mediated restoration of leptin responsiveness in diet-induced obesity: magnitude and mechanisms. *Endocrinology* 149: 5679–5687, 2008.
40. **Turek VF, Trevaskis JL, Levin BE, Dunn-Meynell AA, Irani B, Gu G, Wittmer C, Griffin PS, Vu C, Parkes DG, Roth JD.** Mechanisms of amylin/leptin synergy in rodent models. *Endocrinology* 151: 143–152, 2010.
41. **Unger RH.** Minireview: weapons of lean body mass destruction: the role of ectopic lipids in the metabolic syndrome. *Endocrinology* 144: 5159–5165, 2003.
42. **Wang MY, Chen L, Clark GO, Lee Y, Stevens RD, Ilkayeva OR, Wenner BR, Bain JR, Charron MJ, Newgard CB, Unger RH.** Leptin therapy in insulin-deficient type 1 diabetes. *Proc Natl Acad Sci USA* 107: 4813–4819, 2010.
43. **Weyer C, Maggs DG, Young AA, Kolterman OG.** Amylin replacement with pramlintide as an adjunct to insulin therapy in type 1 and type 2 diabetes mellitus: a physiological approach toward improved metabolic control. *Curr Pharm Des* 7: 1353–1373, 2001.
44. **Young AA, Gedulin B, Vine W, Percy A, Rink TJ.** Gastric emptying is accelerated in diabetic BB rats and is slowed by subcutaneous injections of amylin. *Diabetologia* 38: 642–648, 1995.
45. **Young AA, Gedulin BR, Rink TJ.** Dose-responses for the slowing of gastric emptying in a rodent model by glucagon-like peptide (7–36) NH2, amylin, cholecystokinin, and other possible regulators of nutrient uptake. *Metabolism* 45: 1–3, 1996.

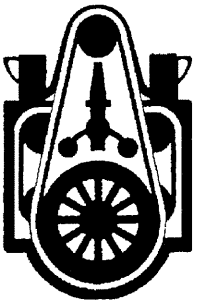

⌘ *Author's Choice*

THE JOURNAL OF BIOLOGICAL CHEMISTRY VOL. 287, NO. 8, pp. 5710–5719, February 17, 2012

Role of Novel Rat-specific Fc Receptor in Macrophage Activation Associated with Crescentic Glomerulonephritis*

Received for publication, May 13, 2011, and in revised form, October 27, 2011 Published, JBC Papers in Press, December 19, 2011, DOI 10.1074/jbc.M111.260695

Theresa H. Page[‡], Zelpha D'Souza[§], Satoshi Nakanishi[¶], Tadao Serikawa[¶], Charles D. Pusey[‖], Timothy J. Aitman[§], H. Terence Cook[**], and Jacques Behmoaras[1]**

From the [‡]Kennedy Institute of Rheumatology Division, Imperial College London, London W6 8LH, United Kingdom, the [§]Medical Research Council Clinical Sciences Centre, the [‖]Renal Department, and the [**]Centre for Complement and Inflammation Research Imperial College London, Hammersmith Hospital, W12 0NN London, United Kingdom, and the [¶]Institute of Laboratory Animals, Graduate School of Medicine, Kyoto University, Yoshidakanoe-cho, Sakyo-ku, Kyoto 606-8501, Japan

Background: Fc receptor-mediated macrophage activation is a major cause of glomerular damage in crescentic glomerulonephritis.
Results: We investigated the role of a novel rat Fc receptor, Fcgr3-rs, in human and rat macrophage activation.
Conclusion: We showed that this receptor prevents the cell signaling of its paralogue (Fcgr3).
Significance: These results provide a novel way to inhibit Fc receptor-mediated cell activation in macrophages.

Crescentic glomerulonephritis (Crgn) is a complex disease where the initial insult is often the glomerular deposition of antibodies against intrinsic or deposited antigens in the glomerulus. The role of Fc receptors in the induction and progression of Crgn is increasingly recognized, and our previous studies have shown that copy number variation in Fcgr3 partially explains the genetic susceptibility of the Wistar-Kyoto (WKY) rat to nephrotoxic nephritis, a rat model of Crgn. The Fcgr3-related sequence (Fcgr3-rs) is a novel rat-specific Fc receptor with a cytoplasmic domain 6 amino acids longer than its paralogue, Fcgr3. The Fcgr3-rs gene is deleted from the WKY rat genome, and this deletion is associated with enhanced macrophage activity in this strain. Here, we investigated the mechanism by which the deletion of Fcgr3-rs in the WKY strain leads to increased macrophage activation. By lentivirus-mediated gene delivery, we generated stably transduced U937 cells expressing either Fcgr3-rs or Fcgr3. In these cells, which lack endogenous Fcgr3 receptors, we show that Fcgr3-rs interacts with the common Fc-γ chain but that Fc receptor-mediated phagocytosis and signaling are defective. Furthermore, in primary macrophages, expression of Fcgr3-rs inhibits Fc receptor-mediated functions, because WKY bone marrow-derived macrophages transduced with Fcgr3-rs had significantly reduced phagocytic activity. This inhibitory effect on phagocytosis was mediated by the novel cytoplasmic domain of Fcgr3-rs. These results suggest that Fcgr3-rs may act to inhibit Fcgr3-mediated signaling and phagocytosis and could be considered as a novel mechanism in the modulation of Fc receptor-mediated cell activation in autoimmune diseases.

In crescentic glomerulonephritis, leukocytes, especially monocytes/macrophages, infiltrating the glomerulus play a critical role in the development of the disease by recognizing immunoglobulins and complement factors via cell surface receptors (1). One of the checkpoints regulating the immune response in glomerular inflammation is through leukocyte cell surface receptors for the Fc (fragment crystallizable) portion of IgG. The family of Fc receptors can regulate the fine balance between pro-inflammatory *versus* anti-inflammatory states of cell activation, and there is increasing evidence suggesting that genetic susceptibility to autoimmune diseases is partly dependent on Fc receptor-mediated activating and inhibitory signaling pathways determining the net signal (pro- or anti-inflammatory) in the progression of the disease (2, 3). In systemic lupus erythematosus, aberrant expression or the presence of allelic variants of FcγRs with altered functionality have been reported to contribute to the pathogenesis of the disease (4).

There are two distinct classes of Fc receptors: the activatory and the inhibitory receptors. Most activatory receptors serve as the ligand-binding component of a receptor that also includes a signal transducing molecule containing an immunoreceptor tyrosine-based activation motif (ITAM)[2] (5). In monocytes and macrophages, this role is fulfilled by the common γ chain. Signaling via its ITAM motif triggers the activation of multiple downstream signaling pathways including the activation of Src and Syk kinases, calcium mobilization, and NF-κB activation, leading ultimately to cellular responses such as phagocytosis and cytokine production. The importance of activatory Fcγ receptors in glomerulonephritis has been shown using mice engineered to lack the ITAM-bearing Fc receptor γ chain. We and others have shown that these mice are protected from glomerulonephritis induced by antibodies to glomerular basement membrane (6–8). In contrast, the inhibitory Fc receptor FcγRIIB has an immunoreceptor tyrosine-based inhibitory

* This work was supported by intramural funding from the Wellcome Trust, Clinical Sciences Centre, and the United Kingdom Medical Research Council. Recipient of an Imperial College Junior Research Fellowship.
⌘ *Author's Choice*—Final version full access.
[1] To whom correspondence should be addressed: Centre for Complement and Inflammation Research, Imperial College London, Hammersmith Hospital, Du Cane Rd., W12 0NN London, UK. Tel.: 44-20-8383-2339; Fax: 44-20-8383-8577; E-mail: Jacquesb@imperial.ac.uk.

[2] The abbreviations used are: ITAM, immunoreceptor tyrosine-based activation motif; FcR, Fc receptor; BMDM, bone marrow-derived macrophage; NTN, nephrotoxic nephritis; Crgn, Crescentic glomerulonephritis; WKY, Wistar-Kyoto; qRT, quantitative RT; PMA, phorbol 12-myristate 13-acetate.

motif and does not use the common γ chain (3). Activatory and inhibitory Fcγ receptors are often expressed on the same cell, and when co-aggregated by IgG antibody, the net signal to the cell depends on the sum total of the activator and inhibitor signals, thus setting thresholds for effector cell responses (3).

In our previous studies of nephrotoxic nephritis (NTN), a model of crescentic glomerulonephritis in the Wistar-Kyoto (WKY) rat, we performed genome-wide linkage analysis for glomerular crescents, macrophage infiltration, and proteinuria in an F2 population derived from NTN-susceptible WKY and NTN-resistant Lewis rats (9). The most significant linkage (logarithm of odds > 8) was obtained with a quantitative trait locus mapping to chromosome 13 (*Crgn1*) accounting, respectively, for 21.8, 16.7, and 12.9% of the genetic variance in crescent formation, proteinuria, and macrophage infiltration. Positional cloning of *Crgn1* led to the identification and functional characterization of the *Fcgr3*-related sequence (*Fcgr3-rs*), a novel rat-specific activatory Fc receptor arising from copy number variation in the *Fcgr3* gene (9). The genomic rearrangement in the *Fcgr3* gene is such that there is a duplication of exon 5 in the NTN-resistant Lewis genomic DNA with the presence of a shorter exon lacking a sequence of 226 bp in its 3′-untranslated region. This shorter exon 5 was deleted in the WKY genome, suggesting a copy number variation in the *Fcgr3* gene. Sequence analysis of this shorter copy of exon 5 revealed deletion of a single guanine nucleotide at position 129 (ΔG129) in the coding sequence of the cytoplasmic domain, resulting in a frameshift and generating a novel cytoplasmic domain 6 amino acids longer than that encoded by *Fcgr3*. We designated this copy number variant *Fcgr3*-related sequence (*Fcgr3-rs*) and showed that this novel variant is transcribed and translated in the Lewis strain, whereas it is deleted from the WKY genome (9).

Given the increased macrophage activity and associated NTN susceptibility in the WKY rat that lacks the Fcgr3-rs molecule, it is important to understand how the presence of this molecule might be influencing macrophage activity. Thus, we have studied the role of *Fcgr3-rs* in macrophage activation. We first investigated whether the genomic duplication/deletion event giving rise to *Fcgr3-rs* occurred during the derivation of inbred Wistar-related colonies. We have then generated U937 cells stably expressing either *Fcgr3* or *Fcgr3-rs* and have studied the role of *Fcgr3*-rs in macrophage activation both in U937 cells and WKY bone marrow-derived macrophages (BMDMs) transduced with *Fcgr3-rs*. Our results show that the absence of Fcgr3-rs is not specific to the WKY strain but is widely distributed throughout the rat phylogenetic tree. Furthermore, in both human monocyte cell lines and primary rat macrophages, expression of *Fcgr3-rs* inhibits *Fcgr3*-mediated signaling and phagocytosis, suggesting that the rat possesses a unique mechanism by which Fc receptor-mediated cell activation can be modulated.

EXPERIMENTAL PROCEDURES

Animals—WKY (WKY/NCrl) rats were purchased from Charles River. All of the procedures were performed in accordance with the United Kingdom Animals (Scientific Procedures) Act.

Reagents—RPMI 1640 containing 25 mM L-glutamine was purchased from Biowhittaker (Berkshire, UK). FCS was from PAA (Yeovil, UK) or Labtech (East Sussex, UK). All of the growth media were supplemented with penicillin (100 units/ml) and streptomycin (100 μg/ml), supplied as a 100× sterile solution from Biowhittaker. LPS was obtained from Sigma. Antibodies were from Millipore (anti-Myc), Santa Cruz ($F(ab')_2$, anti-Syk, anti-CD16), GE Healthcare (HRP-conjugated antibodies for Western blot), or Upstate Biotech (anti-γ chain). pCSGW vector was a gift from Richard Jenner (University College London, London, UK).

Fcgr3 Exon 5 Genotyping—*Fcgr3* exon 5 genotype was determined by PCR and agarose gel electrophoresis by using primers to amplify exon 5 genomic DNA from 134 laboratory rat strains and substrains available in the National BioResource project for the rat in Japan. The primer sequence used is as follows: 5′-GTCCCTAAATTCTGAATTTC-3′ and 5′-AAAGAAGTCACAGAAAGGAG-3′.

Lentiviral Constructs—*Fcgr3* and *Fcgr3-rs* were amplified from Lewis spleen cDNA with forward primer 5′-AAGCTTGCCACCATGACTTTGGAG-3′ and reverse primer 5′-TCTAGATTATTAGCCATACGATGGGAT-3′. Clones were reamplified with forward primer 5′-CGGAAGCTTGCCACCATGGAGCAGAAACTCATCTCTGAAGAGGATCTGACTTTGGAGACCCAGATGTTTCAG-3′ and reverse primer 5′-CCTTGAGCACCTGGATCCATGGGG-3′ and recloned. Site-directed mutagenesis was performed on the Fcgr3 construct for ΔG129 with primers 5′-GAGAAATCTTCAAACCTCGGGGAGGACTGGAGGAAATCCC-3′ (forward) and 5′-GGGATTTCCTCCAGTCCTCCCCGAGGTTTGAAGATTTCTC-3′ (reverse). All α subunit constructs were cloned into the pcDNA3.1/Hygro(+) expression vector (Invitrogen). For inserting an N-terminal Myc tag into the *Fcgr3* constructs, 1.0 μg of the *Fcgr3*, *Fcgr3-rs*, and *Fcgr3*-ΔG constructs were amplified with forward primer 5′-CGGAAGCTTGCCACCATGGAGCAGAAACTCATCTCTGAAGAGGATCTGACTTTGGAGACCCAGATGTTTCAG-3′ and reverse primer 5′-CCTTGAGCACCTGGATCCATGGGG-3′. Constructs and PCR products were cut with HindIII and BamHI and ligated to each other. Lentivirus constructs were prepared as follows: DNA was excised from pCDNA3.1 by digestion with HindIII/XbaI, and blunt ends were created using *Pfu* DNA polymerase. This was ligated into a SmaI cut pENTR4.3F. This "in house" modified version of the pENTR4 gateway vector contains a multiple cloning site downstream of a CMV promoter and upstream of an internal ribosome entry sequence, which mediates expression of an enhanced GFP sequence. Inserts in the correct orientation were identified by diagnostic restriction enzyme digests. Subsequent digestion of this vector with SalI and NotI released a DNA "cassette" containing the "gene of interest" internal ribosome entry sequence-EGP sequences. This was then cloned into the pCSGW lentiviral transfer vector (10) following removal of the vectors own GFP sequence.

Lentiviral Production and Titration—Transfer vector (pCSGW), lentiviral mammalian expression vector (envelope, pMD2.G), and packaging vector (psPAX2) were mixed at a ratio of 4:3:1 and used to infect confluent monolayers of 293T17 cells by calcium phosphate precipitation. The medium was replaced

after 16 h. Media containing virus were collected after a subsequent 24 and 48 h of culture. Insoluble debris was removed by centrifugation and sterilized by filtration through 0.2-μ filters. This crude viral supernatant was stored at −80 °C until use. Titers of viral preparations produced in this way were established by infection of U937 cells as follows. Briefly, U937 cells were mixed with varying dilutions of viral supernatant (typically 1/5 to 1/500) in the presence of 8 mg/ml polybrene (hexadimethrine bromide; Sigma). The cells were "spinoculated" by spinning at 2200 rpm for 2 h at 30 °C. After 72 h, the percentage of GFP-positive cells (FITC channel) was determined by FACS analysis (using a LSRII FACS). The lowest dilution factor with GFP+ score of <20% was used to calculate viral titer.

U937 Lentiviral Line Production—Human monoblastic leukemia U937 cells were infected with lentivirus carrying the gene of interest at a ratio of 1:1 (cells:virus) as described above. The cells were then cultured overnight before removal of virus containing media. Cell surface Myc-positive cells (Myc-Fcgr3 or Myc-Fcgr3RS) were isolated by panning on 10-cm Petri dishes coated with anti-Myc antibody (Millipore). Adherent cells were expanded in culture and used in subsequent experiments. GFP-positive cells expressing pCSGW (no surface Myc) were isolated by cell sorting based on FITC fluorescence. Subsequent analysis of cell lines by FACS analysis confirmed 90–100% of cells to be FITC-positive.

FcR Stimulation—The cells were resuspended in ice-cold serum-free RPMI and anti-Myc antibody (Millipore) added to a final concentration of 130 μg/ml. After 60 min of incubation on ice, the cells were washed three times and resuspended in serum free RPMI with 8 mg/ml goat anti-mouse IgGF(ab')$_2$. The cells were then incubated at 37 °C for the indicated times. The reaction was stopped by the addition of gel sample buffer (2% SDS, 10% glycerol, 0.5% β-mercaptoethanol, 50 mM Tris, pH 6.8).

Immunoprecipitations and Western Blot Analysis—The cells were lysed in ice-cold lysis buffer (25 mM Tris, pH 7.6, 150 mM NaCl, 1 mM EDTA, 0.1% Triton X-100, pH 7.8, 1% digitonin), containing protease inhibitor mixture (Sigma) with 1 mM DTT, 10 mM NaF, 100 mM sodium orthovanadate). The nuclei and cell debris were removed by centrifugation, and supernatants were precleared with protein G-Sepharose. Myc-labeled proteins were then precipitated with anti-Myc antibody (Millipore) or isotype matched control antibody and protein G-Sepharose for 1.5 h. Immunoprecipitated complexes were washed in lysis buffer and were resolved on 4–20% SDS-PAGE gels (Criterion).

After electrotransfer on to nitrocellulose membrane, the membranes were blocked in 2% BSA/TBS/Tween (0.05%) and probed with the appropriate antibodies at 4 °C overnight followed by HRP-conjugated secondary antibody. Blots were developed using ECL (Amersham Biosciences).

ELISAs—At 24 h after stimulation, the supernatants were harvested. The concentrations of TNFα and IL-10 were determined by ELISA (PharMingen) according to the manufacturer's instructions. Absorbance was read and analyzed at 450 nm on a spectrophotometric ELISA plate reader (Labsystems Multiskan Biochromic) using the Ascent software program.

BMDM Preparation and Phagocytosis Assay—Femurs from adult WKY rats were isolated and flushed with Hanks' balanced salt solution. Total BM-derived cells were plated and infected with lentivirus carrying the gene of interest at a ratio of 5:1 (cells: virus). 48 h following the infection, the medium was replaced with DMEM that contained 25 mM HEPES (Sigma), 25% L929 conditioned medium, 25% decomplemented FBS (Biosera), penicillin (100 units/ml; Invitrogen), streptomycin (100 μg/ml; Invitrogen), and cultured for 5 days. These cells were characterized as macrophages by ED-1 staining. To assess phagocytosis, latex polystyrene 6.0-μm microspheres (50 beads/macrophage; Polysciences Inc.) were opsonized with BSA-anti-BSA IgG (Sigma) and added to transduced WKY macrophages cultured in 8-well glass chamber slides. Following staining with Diff-Quick fix (Dade Behring), 200 macrophages were counted to determine the number of beads ingested per cell.

Expression Analysis by qRT-PCR—Stably transduced U937 cells were differentiated in macrophages after adding PMA (100 nM) for 48 h and stimulated with LPS (Sigma; 1 μg/ml) for 3 h. Total RNA was extracted using TRIzol (Invitrogen), and one-step qRT-PCR was performed using 100 ng of total RNA and Brilliant II SYBR® Green QRT-PCR Master Mix Kit (Agilent) with specific primers for *Tnfa* and *IL1b1* in an ABI 7900 sequence detection system (Applied Biosystems, Warrington, UK). In rat BMDMs, Fcgr3 levels relative to total Fcgr3 (Fcgr3 + Fcgr3-rs) were assessed by selecting a forward primer where Fcgr3 differs from Fcgr3-rs by two single nucleotide polymorphisms at the end of the 3'-end. The selected primers were Fcgr3-Forward: 5'TCTAGTGTGGTTCCATGCCG-3' and Fcgr3-Reverse: 5'-TGTCCTGTGGAGCCTTGTACT-3'; total Fcgr3 (Fcgr3+Fcgr3-rs)-Forward: 5'-CTCCAGACCCCTCAACTGGT-3' and total Fcgr3 (Fcgr3+Fcgr3-rs)-Reverse: 5'-GCAGTAGTAGTTCCCACTGT-3'.

Statistical Analysis—Statistical differences in mean values were compared using one-way analysis of variance followed by Dunnett's multiple comparison post-test; $p < 0.05$ was considered statistically significant.

RESULTS

The Phylogeny of Genomic Deletion of Fcgr3-rs in Laboratory Rat—Exon 5 of *Fcgr3-rs* contains a deletion of a single guanine nucleotide at position 129 (ΔG129) in the coding sequence of the cytoplasmic domain (9). When compared with *Fcgr3*, this ΔG129 variant results in a frameshift in the *Fcgr3-rs* coding sequence and generates a novel cytoplasmic domain 6 amino acids longer than that encoded by *Fcgr3* that was not found in any other species (Fig. 1). We have previously shown that Fcgr3-rs was deleted from NTN-susceptible Kyoto-derived strains (9), but to investigate the distribution of this deletion throughout the rat genealogical tree, we carried out a phylogenetic tree analysis of 94 inbred laboratory strains and 40 of their substrains (Fig. 2). The results show that the deletion of *Fcgr3-rs* is widespread throughout the rat phylogeny (32 of 94 strains), suggesting that the origin of the deletion event is earlier then the derivation of these strains. We also investigated the relative levels of Fcgr3 and Fcgr3-rs mRNA levels in Lewis rat BMDMs by qRT-PCR and showed that although there is relatively

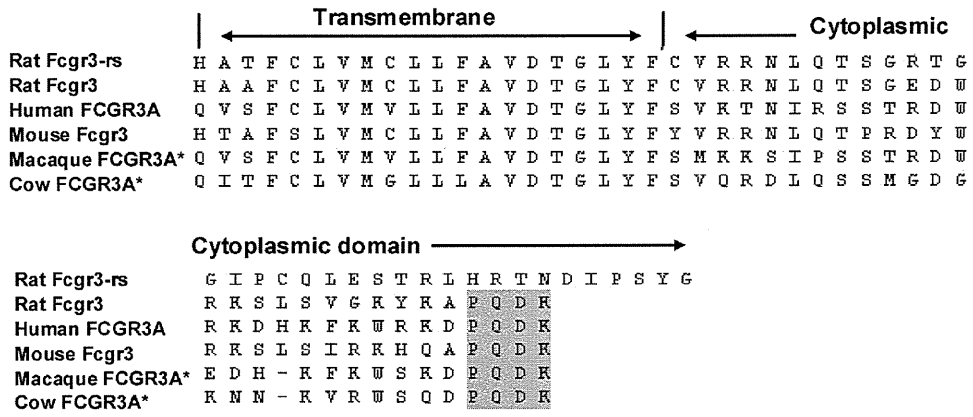

FIGURE 1. **Rat-specific *Fcgr3-rs* is a novel Fc receptor with a unique cytoplasmic domain 6 amino acids longer then *Fcgr3*.** Shown is a comparison of amino acid sequences of transmembrane and cytoplasmic domains of rat *Fcgr3* and *Fcgr3-rs*, human *Fcgr3*, and FCGR3 in other species. Fcgr3-rs has lost the terminal PQDK sequence (*highlighted*) that is highly conserved across species. *, amino acid prediction based on human FCGR3A using Ensembl Genome Browser.

increased Fcgr3 expression when compared with Fcgr3-rs, LPS stimulation did not change the relative levels of both receptors (Table 1).

U937 Cells Expressing Either Fcgr3 or Fcgr3-rs: Surface Expression and Interaction with γ Chain—The U937 cell line does not express any endogenous FcgRIIIA (11) and is therefore an ideal tool for the analysis of FcgRIII receptors, allowing direct functional comparison between the rat orthologues Fcgr3 and Fcgr3-rs. Thus, to study the role of *Fcgr3-rs* in macrophage activation, we generated U937 cells stably transduced with lentivirus constructs expressing the protein of interest. U937 cells were infected with either Myc-tagged Fcgr3 (Myc-Fcgr3), Myc tagged-Fcgr3-rs (Myc-Fcgr3RS), or empty (pCSGW) lentiviral vectors. All of the lentiviral vectors contained GFP. Expression of Myc-Fcgr3 and Myc-Fcgr3-rs was confirmed by fluorescence microscopy, detecting GFP+ cells and also by a Myc Western blot on lysates from stably transduced U937 cells (Fig. 3*A*). We then investigated whether Myc-Fcgr3 and Myc-Fcgr3-rs are expressed on the surface of U937 cells. Flow cytometry analysis using an anti-Myc-APC mouse antibody (mAb) showed that both Myc-Fcgr3 and Myc-Fcgr3-rs are expressed on the cell surface at similar levels in these cells (Fig. 3*B*). Because Fcgr3 transport to and expression at the cell surface is known to be dependent on its association with the common γ chain (12), these findings implied that both the Fcgr3 and Fcgr3-rs molecules were associated with γ chain at the cell surface. Co-immunoprecipitation analysis of U937 cells expressing either Fcgr3 or Fcgr3-rs demonstrated that this was indeed the case (Fig. 3*C*). Thus, although Fcgr3-rs has an additional cytoplasmic domain 6 amino acids longer than its paralogue Fcgr3, it binds the γ-chain on the surface of stably transduced and PMA-differentiated U937 macrophages.

Fcgr3-rs-mediated Signaling and Phagocytosis in U937 Cells—In most macrophage Fc receptor complexes (with the exception of FcgrII), the ITAM-containing common γ-chain is necessary for downstream signaling (13, 14). Thus, the dimeric γ-chain forms multichain complexes with the ligand binding α-chain of Fcgr3 to allow signal transduction (3). This signaling starts with tyrosine phosphorylation of the ITAMs by kinases of the SRC family (15, 16) and leads to the recruitment and subsequent phosphorylation of the Syk kinase, followed by the activation of various downstream targets such as PI3K and NF-κB. Subesquent changes in gene expression led to the induction of inflammatory cytokines such as TNFα. We were therefore keen to understand whether the Fcgr3-rs is able to transduce signals similar to those described for Fcgr3. However, despite its interaction with the γ-chain, cross-linking of Fcgr3-rs with anti-Myc antibody does not lead to phosphorylation of Syk or the degradation of IκBα (Fig. 4*A*). This was not the case for the U937 macrophages stably transduced with Fcgr3 (Fig. 4*A*).

Furthermore, Fc receptor-mediated TNFα production and IgG-opsonized bead phagocytosis were also significantly less in U937 macrophages expressing Fcgr3-rs when compared with U937 macrophages stably transduced with Fcgr3 (Fig. 4*B*). Taken together, these results suggest that the rat-specific Fcgr3-rs is unable to mediate the same intracellular signals as the wild type receptor.

Fcgr3-rs-and TLR4-mediated TNFα and IL-1β Expression Levels—To test whether the relative reduction in TNFα production in U937 cells transduced with Myc-Fcgr3RS is specific to receptor cross-linking, we have stimulated the stably transduced PMA-differentiated U937 cells with LPS for 3 h and measured TNFα and IL-1β expression levels by qRT-PCR (Fig. 5). Although the results have confirmed the previously shown up-regulation of these genes in U937 cells (17), there was no significant difference in the up-regulation of TNFα and IL-1β between U937 + Myc-Fcgr3 and U937 + Myc-Fcgr3RS, demonstrating that the inability of these cells to produce TNFα is not an intrinsic property of these cells and is specific to Fcgr3 stimulation (Fig. 5).

The Role of the Novel Cytoplasmic Domain of Fcgr3-rs in Rat and Human Macrophage Activation—To study the effect of Fcgr3-rs on the phagocytic activity of primary WKY BMDMs where other endogenous, FcRs (Fcgr3 and others) are expressed, we transduced these cells with lentivirus encoding either Myc-Fcgr3rs or Myc-Fcgr3 and used cells transduced with the empty vector (pCSGW) as controls.

Because the Fcgr3-rs also contains a number of single-base pair substitutions in its extracellular domain, we were also keen to establish whether these might explain the differences between the related sequence and wild type Fcgr3 molecules, possibly as a

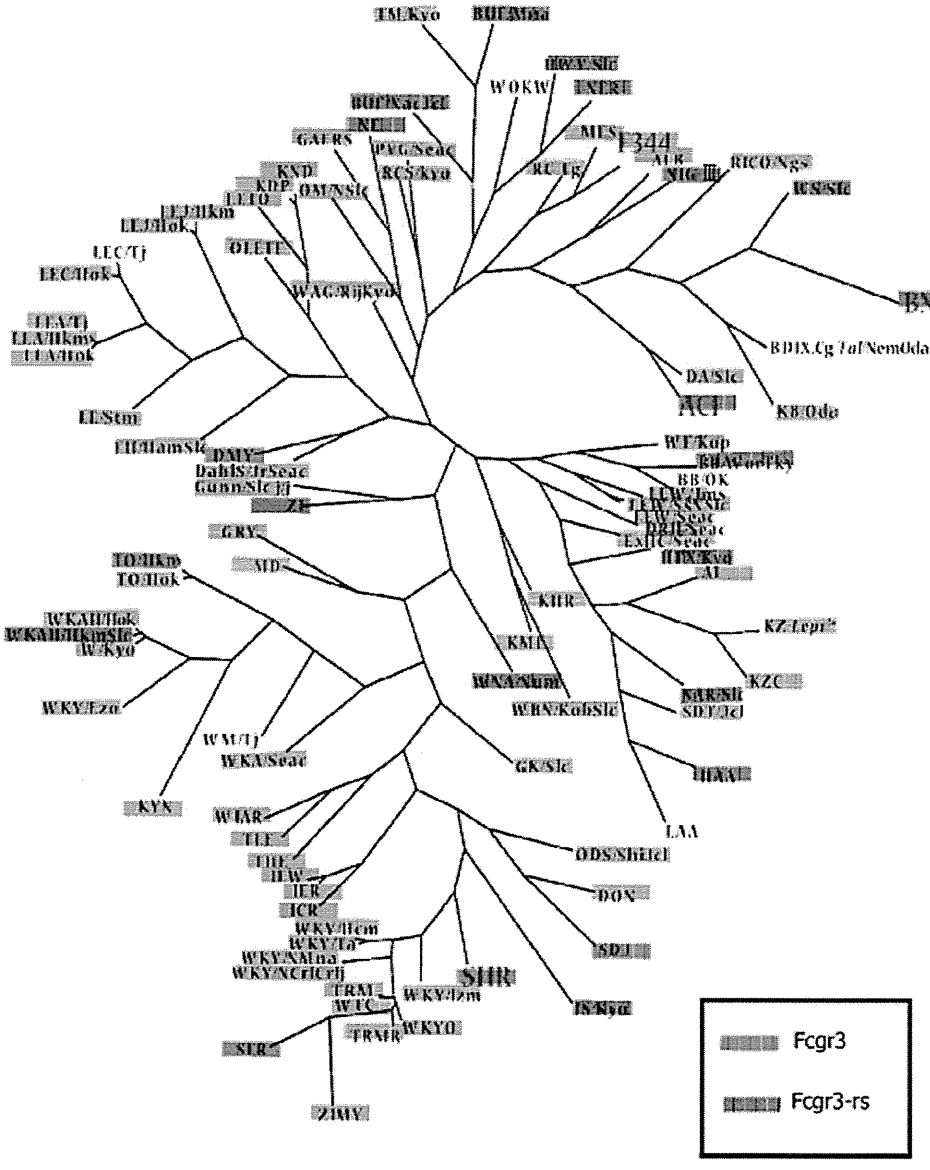

FIGURE 2. **Phylogenetic tree of 134 laboratory rat strains according to the presence or absence of *Fcgr3-rs* in the genome.** A phylogenetic tree of 94 strains is shown. Strains having numerous substrains (*i.e.* SHR, F344) are shown in capital letters, and all of the substrains showed the same genotype as the founder strain. The tree was developed through a heuristic search for maximum parsimony implemented in PAUP 4.0b10. TreeView was used to display the radial tree. For BD IX, LEC/Tj, and WM/Tj, genotypes could not be determined.

TABLE 1

Relative mRNA levels of Fcgr3 and Fcgr3-rs in Lewis rat BMDMs

Expression was assessed by qRT-PCR with specific primers that differentiate between Fcgr3 and Fcgr3-rs in basal and LPS-stimulated (100 ng/ml, for 5 h) BMDMs. Fcgr3 and Fcgr3-rs expression levels were normalized to total Fcgr3 (Fcgr3 + Fcgr3-rs) levels.

	BMDM	
Expression	Basal	LPS
Fcgr3/(Fcgr3 + Fcgr3-rs)	0.73 ± 0.02	0.67 ± 0.01
Fcgr3-rs/(Fcgr3 + Fcgr3-rs)	0.27 ± 0.02	0.33 ± 0.01

result of altered FcR binding. Thus, we also generated an additional lentiviral construct encoding a chimeric protein to specifically test the effect of the novel cytoplasmic domain of Fcgr3-rs on Fc receptor-mediated phagocytosis. Fcgr3-ΔG contains the wild type Fcgr3 extracellular, transmembrane, and cytoplasmic domains with the presence of the Fcgr3-rs-specific novel cytoplasmic domain (9) (Fig. 6*A*).

We first measured the expression of Fcgr3 by using primers specific for the transmembrane domain, thereby allowing differential amplification between *Fcgr3* and *Fcgr3-rs* transcripts (Fig. 6*B*). We then measured the number of opsonized beads phagocytosed by 200 WKY BMDMs transduced with each different lentiviral construct.

Phagocytosis was significantly reduced in Fcgr3-rs transduced WKY BMDMs when compared with those transduced with pCSGW (Fig. 6*C*). This inhibitory effect is clearly mediated by the novel cytoplasmic domain of Fcgr3-rs, because similar reductions in phagocytic activity were seen in WKY BMDMs transduced either with Fcgr3-ΔG or with Fcgr3-rs (Fig. 6*C*). Taken together, these data suggest that the presence of FcRs containing the related sequence cytoplasmic domain is able to reduce phagocytosis mediated by endogenous FcRs in the WKY BMDMs.

To further understand the mechanism of action of the Fcgr3-rs, we then investigated how the Fcgr3 and Fcgr3-rs

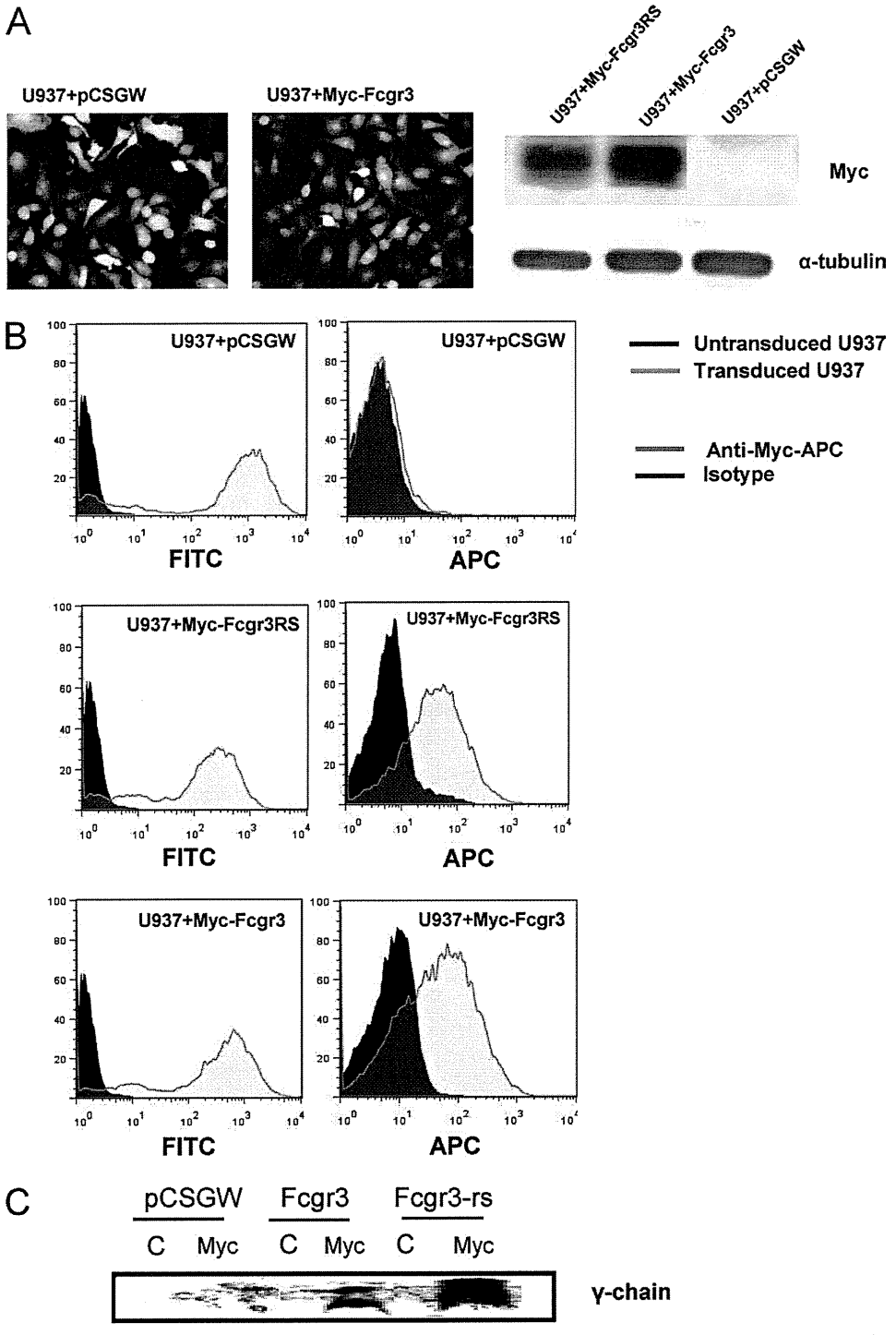

FIGURE 3. **Surface expression of Fcgr3-rs and Fcgr3 and assessment of their interaction with the γ chain in stably transduced U937 cells.** *A*, illustration of GFP expression in U937 + pCSGW and U937 + Myc-Fcgr3 by fluorescent microscopy (×40). Myc and α-tubulin (loading control) Western blots of whole cell lysates from stably transduced U937 cells are shown. *B*, the human monoblastic leukemia cell line U937 was stably transduced to express either Myc-Fcgr3 (U937 + Myc-Fcgr3) or Myc-Fcgr3RS (U937 + Myc-Fcgr3RS) lentiviral constructs co-expressing GFP together with transgene. Untransduced cells (U937) and cells transduced with lentiviral construct expressing GFP alone (without any transgene, U937 + pCSGW) were used as controls. Surface expression was measured by using anti-Myc-APC mAb. All of the transduced cells were GFP+ as shown by FITC emission. *C*, stably transduced U937 cells were differentiated into macrophages after adding PMA (100 nM) for 48 h, and cell lysates were precipitated with anti-Myc antibody. Immunoprecipitated proteins were blotted with anti-γ chain antibody.

interact with TLR4-mediated TNFα production following LPS stimulation. U937 cells transduced with FcRs (U937 + Myc-Fcgr3, U937 + MycFcgr3RS, and U937 + Myc-Fcgr3ΔG) were cross-linked with anti-Myc antibodies and IgG F(ab′)$_2$. Following washing, the cells were stimulated with LPS for 5 h. TNFα and IL-10 protein levels were measured by sandwich ELISA.

In the absence of any additional FcR expression in these cells, treatment with Ab·Fab complexes resulted in a 38% decrease in TNF production. This was further decreased in

the presence of the Fcgr3 molecule to 50% of that seen in cells that are not cross-linked, revealing that signals from Fcgr3 act to reduce TLR4-induced TNF production in U937 cells (Fig. 6*D*). In contrast, the presence of either the Fcgr3-rs or Fcgr3ΔG did not result in any changes in TNFα production compared with cells that are not cross-linked. Levels of IL-10 produced in these cells did not differ significantly between Fcgr3 and FcgR3-rs or FcgR3-ΔG cells (Fig. 6*E*), revealing that the Fcgr3-rs is not functioning in these cells by increasing levels of this anti-inflammatory cytokine.

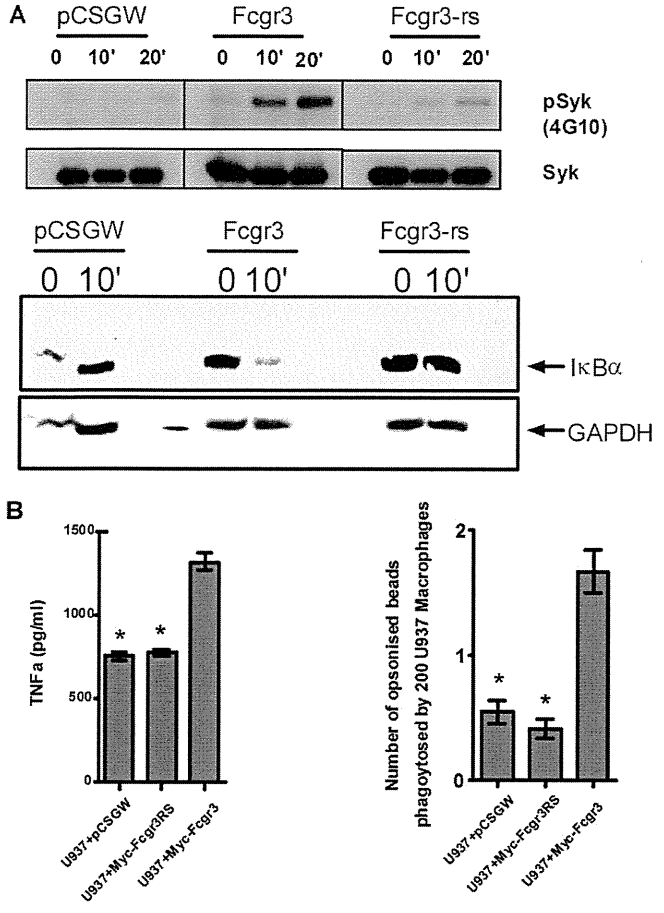

FIGURE 4. **Fc receptor-mediated signaling and phagocytosis in U937 cells stably transduced with Myc-Fcgr3RS.** *A*, Fc receptor stimulation after cross-linking with anti-Myc Ab for a maximum of 20 min and analysis of Syk phosphorylation and IκBα degradation in stably transduced U937-derived macrophages. *B*, TNFα levels were assessed by sandwich ELISA after cross-linking stably transduced U937 macrophages by anti-Myc mAb. Supernatants were collected after 48 h of incubation. Fc receptor-mediated bead phagocytosis was assayed by incubating macrophages with IgG opsonized latex beads. Nonopsonized beads did not show any phagocytosis. *, $p < 0.001$ when compared with U937 + Myc-Fcgr3.

DISCUSSION

There is considerable evidence from experimental models of crescentic glomerulonephritis that Fcγ receptors play a central role in disease progression. In mice, the FcR chain-deficient mice (FcRγ$^{-/-}$) lack surface expression of both murine activator Fc receptors I, III, and IV, and the high affinity IgE receptor (FcRI) (18). Several studies have shown that FcRγ$^{-/-}$ mice are protected from disease in accelerated nephrotoxic nephritis (6, 7, 19), and we have shown that the disease is mediated by Fcγ receptors on circulating leukocytes and not intrinsic renal cells (8). Our previous studies in the NTN model in the Wistar Kyoto rat showed that the disease architecture is complex and highly heritable, with seven quantitative trait loci (*Crgn1–7*) linked to the percentage of glomerular crescents and controlling mainly macrophage activation through distinct transcriptome profiles (9, 20–22). In this model, we showed that copy number variation in rat *Fcgr3* locus led to the deletion of *Fcgr3-rs* in the WKY rat, predisposing this strain to enhanced macrophage activity (9).

The purpose of the current study was to understand the mechanism by which the genomic deletion of *Fcgr3-rs* leads to macrophage overactivation and whether the novel cytoplasmic domain binds to the common γ chain to trigger downstream signaling pathways. We first investigated the distribution of *Fcgr3-rs* deletion throughout the rat phylogeny and found that the deletion was widespread. It was previously reported that five outbred Wistar and one Long-Evans stocks have Fcgr3-rs (23), suggesting that the deletion has originated from the ancestor outbred Wistar colony in the Wistar institute in the United States. We now confirm and extend these findings because all of the laboratory rat strains that we genotyped for Fcgr3 copy

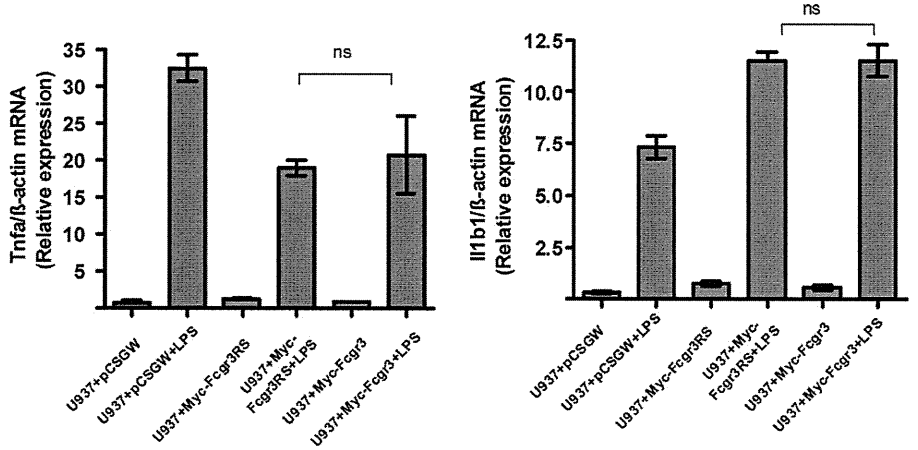

FIGURE 5. **Fcgr3-rs does not affect TLR4-mediated *Tnfa* and *Il1b1* expressions in stably transduced U937 cells.** Stably transduced U937 cells were differentiated in macrophages after adding PMA (100 nM) for 48 h and stimulated with LPS (1 μg/ml) for 3 h. *Tnfa* and *Il1b1* gene expression were measured by qRT-PCR. *ns*, not significant.

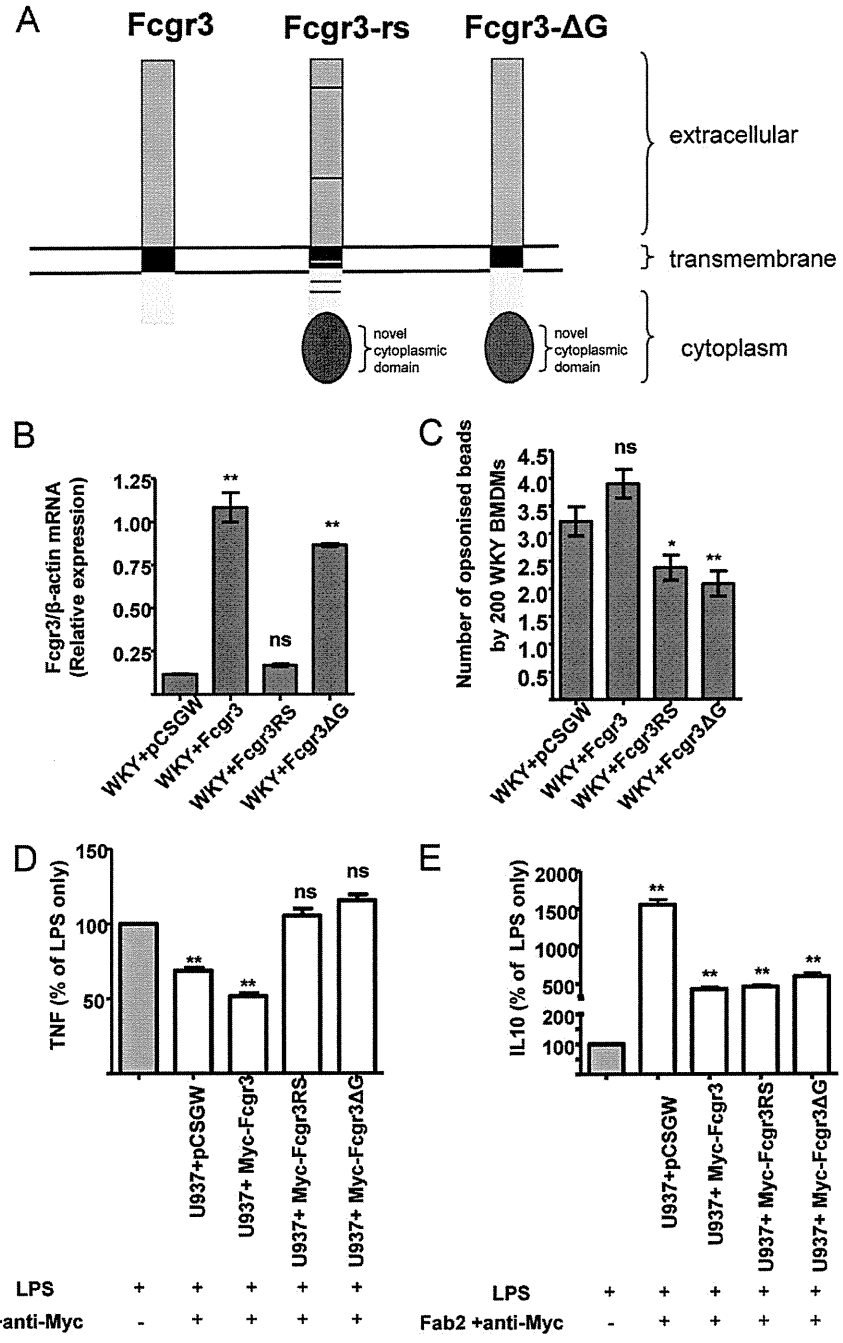

FIGURE 6. **Fcgr3-rs inhibits Fc receptor-mediated phagocytosis in WKY BMDMs.** *A*, schematic representation of the functional differences between Fcgr3 and Fcgr3-rs. Although there are amino acid changes in the Fcgr3-rs extracellular, transmembrane, and cytoplasmic domains (indicated by *bars*) when compared with Fcgr3, the major structural difference is the presence of a novel cytoplasmic domain. The chimeric Fcgr3-ΔG has the extracellular transmembrane and cytoplasmic domains identical to Fcgr3, the only difference being the presence of the novel cytoplasmic domain. *B*, *Fcgr3* expression was assessed by qRT-PCR in stably transduced U937 cells by using specific primers designed based on polymorphisms in the transmembrane domain differentiating between *Fcgr3* and *Fcgr3-rs*. The expression of Myc-Fcgr3 ΔG was also assessed and showed similar expression levels as Fcgr3. This is because Fcgr3 and Fcgr3-ΔG share the same sequence in the transmembrane domain. *C*, WKY bone marrow-derived cells were transduced with lentiviral constructs co-expressing GFP with either Myc-tagged Fcgr3-rs (Myc-Fcgr3RS) or Myc-tagged wild type Fcgr3 (Myc-Fcgr3) or Myc-tagged Fcgr3-ΔG. The lentiviral construct expressing GFP alone (without any transgene) was used as control (pCSGW). The cells were then differentiated into BM-derived macrophages by culturing in DMEM containing L929, and Fc receptor-mediated phagocytosis was performed. **, $p < 0.01$; *, $p < 0.05$; *ns*, not significant when compared with pCSGW. *D* and *E*, LPS-induced TNFα (*D*) and IL-10 (*E*) levels were assessed by sandwich ELISA after cross-linking stably transduced U937 macrophages by anti-Myc mAb and F(ab')$_2$. Following cross-linking, the cells were washed, and supernatants were collected after 5 h of incubation with LPS (1 μg/ml). TNFα and IL-10 production were expressed as a percentage of that produced in LPS-stimulated cells without FcR cross-linking (100% of cytokine production). **, $p < 0.001$ when compared with LPS-stimulated cells without FcR cross-linking (100% of cytokine production; histogram in *gray*)

number variation are derived from outbred Wistar and Long-Evans stocks.

Previously, to investigate how Fcgr3-rs exerts its inhibitory effect on Fcγ receptor signaling, we have transfected COS7 cells and have shown that although Fcgr3-rs is expressed on the cell surface, it is less efficient than Fcgr3 in mediating phagocytosis (9). It also had an inhibitory effect on Fcgr3-mediated phagocytosis when both receptors were co-transfected in COS7 cells

(9). However, the COS7 cells are not primarily phagocytic cells and do not endogenously express the γ chain, making it difficult to draw mechanistic conclusions concerning the role of Fcgr3-rs in Fc receptor-mediated signaling and activation. Here we have examined the signaling function of Fcgr3-rs in a human monocyte cell line U937, a well characterized cell line previously used to study Fc receptor function (11). U937 cells constitutively express only Fcgr1 and Fcgr2a but not Fcgr3 (11). We have used lentivirus-mediated gene transfer to generate stably transduced U937 cell lines. Our results showed that Fcgr3-rs associates with the common γ-chain in these cells, but Fc receptor-mediated signaling and phagocytosis are defective. Importantly, WKY BMDMs transduced with the Fcgr3-rs also showed reduced bead phagocytosis, and this was mediated through the rat-specific novel cytoplasmic domain.

It is well established that the transmembrane domain is required for association with the γ chain and consequently cell surface expression of Fcgr3 (24). Because of the amino acid changes between Fcgr3 and Fcgr3-rs in the transmembrane domains, it could therefore be argued that the amino acid changes simply prevented *Fcgr3-rs* expression. This, however, was not the case, and in both U937 cells and primary rat macrophages, Fcgr3-rs was expressed at the cell surface at similar levels to Fcgr3. The use of the ΔG chimeric molecule, which contains the extracellular and transmembrane domains of Fcgr3 combined with the cytoplasmic domain of Fcgr3-rs, also demonstrates that the differences seen between Fcgr3 and Fcgr3-rs functions are mediated only by the novel cytoplasmic domain of Fcgr3-rs and cannot be explained by point mutations in the extracellular domain of Fcgr3-rs, which might simply have prevented Fc binding of IgG.

The majority of signaling cascades emanating from the Fcgr3 receptor complex are thought to be derived from the γ chain via its ITAM motifs. Thus, removal of the γ chain cytoplasmic domain or mutations of tyrosine residues within the ITAM motifs affects intracellular Ca^{+} levels, PI3K activity and receptor-induced phosphorylation events (25). In particular there is compelling evidence that activation of Syk is essential for subsequent events such as receptor-induced phagocytosis (26, 27). However, the cytoplasmic tail of the Fcgr3 molecule is unlikely to be completely redundant in this process, and Hou *et al.* (28) have suggested that sequences within the cytoplasmic domain of Fcgr3, in particular those close to the transmembrane domain, are required for signaling. Our findings demonstrate that signaling from the Fcgr3-rs is clearly different from that mediated by Fcgr3, because Fcgr3-rs·γ chain complexes do not generate phosphorylated Syk molecules or activate the NF-κB transcription factor that is required for transcription of Fc-responsive genes such as TNFα. Accordingly, IgG-induced TNFα production and phagocytosis are both significantly lower in U937 cells expressing Fcgr3-rs compared with Fcgr3. Moreover, expressing Fcgr3-rs in primary rat WKY BMDMs resulted in lower levels of phagocytosis than cells expressing Fcgr3 alone, suggesting that Fcgr3-rs has an inhibitory effect on Fcgr3-mediated phagocytosis in these cells.

Although the Fcgr3-rs cytoplasmic domain includes a novel sequence with a single tyrosine molecule, this is not an immunoreceptor tyrosine-based inhibitory motif in the same way as that found in the FcgrIIb receptor. Elegant studies by Kim *et al.* (29) have shown that specific regions of the transmembrane region of Fcγ receptors are important for signaling leading to phagocytosis. The same group has provided further evidence on differences in the signaling properties of FcγR1/γ and FcγRIIA such as their interaction with Syk and Src-related tyrosine kinases (30). The region of the cytoplasmic domain shown by Hou *et al.* (28) to be important in signaling is present in the Fcgr3-rs; however, it is possible that the altered sequence of the remainder of the cytoplasmic domain may render this region inaccessible to essential downstream signaling molecules, thereby rendering it inactive. The question of whether the Fcgr3-rs exerts its effects by acting as a decoy receptor, binding immunoglobulins, but not signaling, or whether its novel cytoplasmic domain induces distinct signaling pathways that act to inhibit those from the wt Fcgr3 is therefore an interesting one.

Our demonstration herein that the -rs does not induce Syk or NF-κB activation suggests that this molecule may not signal, and this is underscored by the demonstration that LPS-induced TNF and IL-10 production is unaffected in U937 cells by the presence of the -rs. Taken together, these data add further weight to the argument that Fcgr3-rs is a decoy receptor that is able to bind Fc but unable to signal such that its expression inhibits co-expressed Fc receptor-mediated signaling and cell activation. However, we cannot completely rule out a potential additional role of this receptor, which will lead to inhibition by a novel negative signaling pathway. Investigations into this question are continuing in this laboratory.

In conclusion, our results suggest that the rat-specific *Fcgr3-rs* acts to inhibit *Fcgr3*-mediated signaling and phagocytosis in both rodent and human cells and could be considered as a novel therapeutic mechanism for the modulation of Fc receptor-mediated cell activation in macrophage-mediated diseases such as crescentic glomerulonephritis.

Acknowledgments—We thank Sunil Modi for technical assistance. We are thankful to the National BioResource Project for providing rat strains.

REFERENCES

1. Mason, J. C., and Pusey, C. D. (2008) *The Kidney in Systemic Autoimmune Diseases*, 1st Ed., Elsevier, Amsterdam
2. Nimmerjahn, F., and Ravetch, J. V. (2007) Fc-receptors as regulators of immunity. *Adv. Immunol.* **96,** 179–204
3. Nimmerjahn, F., and Ravetch, J. V. (2008) Fcγ receptors as regulators of immune responses. *Nat. Rev. Immunol.* **8,** 34–47
4. Brown, E. E., Edberg, J. C., and Kimberly, R. P. (2007) Fc receptor genes and the systemic lupus erythematosus diathesis. *Autoimmunity* **40,** 567–581
5. Strzelecka, A., Kwiatkowska, K., and Sobota, A. (1997) Tyrosine phosphorylation and Fcγ receptor-mediated phagocytosis. *FEBS Lett.* **400,** 11–14
6. Park, S. Y., Ueda, S., Ohno, H., Hamano, Y., Tanaka, M., Shiratori, T., Yamazaki, T., Arase, H., Arase, N., Karasawa, A., Sato, S., Ledermann, B., Kondo, Y., Okumura, K., Ra, C., and Saito, T. (1998) Resistance of Fc receptor-deficient mice to fatal glomerulonephritis. *J. Clin. Invest.* **102,** 1229–1238
7. Suzuki, Y., Shirato, I., Okumura, K., Ravetch, J. V., Takai, T., Tomino, Y., and Ra, C. (1998) Distinct contribution of Fc receptors and angiotensin II-dependent pathways in anti-GBM glomerulonephritis. *Kidney Int.* **54,** 1166–1174
8. Tarzi, R. M., Davies, K. A., Robson, M. G., Fossati-Jimack, L., Saito, T.,

Walport, M. J., and Cook, H. T. (2002) Nephrotoxic nephritis is mediated by Fcγ receptors on circulating leukocytes and not intrinsic renal cells. *Kidney Int.* **62,** 2087–2096
9. Aitman, T. J., Dong, R., Vyse, T. J., Norsworthy, P. J., Johnson, M. D., Smith, J., Mangion, J., Roberton-Lowe, C., Marshall, A. J., Petretto, E., Hodges, M. D., Bhangal, G., Patel, S. G., Sheehan-Rooney, K., Duda, M., Cook, P. R., Evans, D. J., Domin, J., Flint, J., Boyle, J. J., Pusey, C. D., and Cook, H. T. (2006) Copy number polymorphism in Fcgr3 predisposes to glomerulonephritis in rats and humans. *Nature* **439,** 851–855
10. Bainbridge, J. W., Stephens, C., Parsley, K., Demaison, C., Halfyard, A., Thrasher, A. J., and Ali, R. R. (2001) *In vivo* gene transfer to the mouse eye using an HIV-based lentiviral vector. Efficient long-term transduction of corneal endothelium and retinal pigment epithelium. *Gene Ther.* **8,** 1665–1668
11. Floto, R. A., Clatworthy, M. R., Heilbronn, K. R., Rosner, D. R., MacAry, P. A., Rankin, A., Lehner, P. J., Ouwehand, W. H., Allen, J. M., Watkins, N. A., and Smith, K. G. (2005) Loss of function of a lupus-associated FcγRIIb polymorphism through exclusion from lipid rafts. *Nat. Med.* **11,** 1056–1058
12. Park, J. G., Isaacs, R. E., Chien, P., and Schreiber, A. D. (1993) In the absence of other Fc receptors, Fc γ RIIIA transmits a phagocytic signal that requires the cytoplasmic domain of its γ subunit. *J. Clin. Invest.* **92,** 1967–1973
13. Lowry, M. B., Duchemin, A. M., Robinson, J. M., and Anderson, C. L. (1998) Functional separation of pseudopod extension and particle internalization during Fc γ receptor-mediated phagocytosis. *J. Exp. Med.* **187,** 161–176
14. Davis, W., Harrison, P. T., Hutchinson, M. J., and Allen, J. M. (1995) Two distinct regions of FC γ RI initiate separate signalling pathways involved in endocytosis and phagocytosis. *EMBO J.* **14,** 432–441
15. Ghazizadeh, S., Bolen, J. B., and Fleit, H. B. (1994) Physical and functional association of Src-related protein tyrosine kinases with Fc γ RII in monocytic THP-1 cells. *J. Biol. Chem.* **269,** 8878–8884
16. Wang, A. V., Scholl, P. R., and Geha, R. S. (1994) Physical and functional association of the high affinity immunoglobulin G receptor (Fc γ RI) with the kinases Hck and Lyn. *J. Exp. Med.* **180,** 1165–1170
17. Sharif, O., Bolshakov, V. N., Raines, S., Newham, P., and Perkins, N. D. (2007) Transcriptional profiling of the LPS induced NF-κB response in macrophages. *BMC Immunol.* **8,** 1
18. Takai, T., Li, M., Sylvestre, D., Clynes, R., and Ravetch, J. V. (1994) FcR γ chain deletion results in pleiotrophic effector cell defects. *Cell* **76,** 519–529
19. Wakayama, H., Hasegawa, Y., Kawabe, T., Hara, T., Matsuo, S., Mizuno, M., Takai, T., Kikutani, H., and Shimokata, K. (2000) Abolition of anti-glomerular basement membrane antibody-mediated glomerulonephritis in FcRγ-deficient mice. *Eur. J. Immunol.* **30,** 1182–1190
20. Behmoaras, J., Bhangal, G., Smith, J., McDonald, K., Mutch, B., Lai, P. C., Domin, J., Game, L., Salama, A., Foxwell, B. M., Pusey, C. D., Cook, H. T., and Aitman, T. J. (2008) Jund is a determinant of macrophage activation and is associated with glomerulonephritis susceptibility. *Nat. Genet.* **40,** 553–559
21. Behmoaras, J., Smith, J., D'Souza, Z., Bhangal, G., Chawanasuntoropoj, R., Tam, F. W., Pusey, C. D., Aitman, T. J., and Cook, H. T. (2010) Genetic loci modulate macrophage activity and glomerular damage in experimental glomerulonephritis. *J. Am. Soc. Nephrol.* **21,** 1136–1144
22. Maratou, K., Behmoaras, J., Fewings, C., Srivastava, P., D'Souza, Z., Smith, J., Game, L., Cook, T., and Aitman, T. (2011) Characterization of the macrophage transcriptome in glomerulonephritis-susceptible and -resistant rat strains. *Genes Immun.* **12,** 78–89
23. Kuramoto, T., Nakanishi, S., and Serikawa, T. (2008) Functional polymorphisms in inbred rat strains and their allele frequencies in commercially available outbred stocks. *Physiol. Genomics* **33,** 205–211
24. Lanier, L. L., Yu, G., and Phillips, J. H. (1991) Analysis of Fc γ RIII (CD16) membrane expression and association with CD3 ζ and Fc epsilon RI-γ by site-directed mutation. *J. Immunol.* **146,** 1571–1576
25. Indik, Z. K., Park, J. G., Hunter, S., and Schreiber, A. D. (1995) The molecular dissection of Fc γ receptor mediated phagocytosis. *Blood* **86,** 4389–4399
26. Crowley, M. T., Costello, P. S., Fitzer-Attas, C. J., Turner, M., Meng, F., Lowell, C., Tybulewicz, V. L., and DeFranco, A. L. (1997) A critical role for Syk in signal transduction and phagocytosis mediated by Fcγ receptors on macrophages. *J. Exp. Med.* **186,** 1027–1039
27. Wirthmueller, U., Kurosaki, T., Murakami, M. S., and Ravetch, J. V. (1992) Signal transduction by Fc γ RIII (CD16) is mediated through the γ chain. *J. Exp. Med.* **175,** 1381–1390
28. Hou, X., Dietrich, J., and Geisler, N. O. (1996) The cytoplasmic tail of FcγRIIIAα is involved in signaling by the low affinity receptor for immunoglobulin G. *J. Biol. Chem.* **271,** 22815–22822
29. Kim, M. K., Huang, Z. Y., Hwang, P. H., Jones, B. A., Sato, N., Hunter, S., Kim-Han, T. H., Worth, R. G., Indik, Z. K., and Schreiber, A. D. (2003) Fcγ receptor transmembrane domains: role in cell surface expression, γ chain interaction, and phagocytosis. *Blood* **101,** 4479–4484
30. Huang, Z. Y., Hunter, S., Kim, M. K., Chien, P., Worth, R. G., Indik, Z. K., and Schreiber, A. D. (2004) The monocyte Fcγ receptors FcγRI/γ and FcγRIIA differ in their interaction with Syk and with Src-related tyrosine kinases. *J. Leukoc. Biol.* **76,** 491–499

http://www.kidney-international.org

Pleiotrophin triggers inflammation and increased peritoneal permeability leading to peritoneal fibrosis

Hideki Yokoi[1,2], Masato Kasahara[1,2], Kiyoshi Mori[1], Yoshihisa Ogawa[1], Takashige Kuwabara[1], Hirotaka Imamaki[1], Tomoko Kawanishi[1], Kenichi Koga[1], Akira Ishii[1], Yukiko Kato[1], Keita P. Mori[1], Naohiro Toda[1], Shoko Ohno[1], Hisako Muramatsu[3], Takashi Muramatsu[4], Akira Sugawara[1], Masashi Mukoyama[1] and Kazuwa Nakao[1]

[1]Department of Medicine and Clinical Science, Kyoto University Graduate School of Medicine, Kyoto, Japan; [2]Division of Nephrology and Blood Purification, Kobe Institute of Biomedical Research and Innovation, Hyogo, Japan; [3]Department of Health and Nutrition, Faculty of Psychological and Physical Science, Aichi Gakuin University, Aichi, Japan and [4]Department of Health Science, Faculty of Psychological and Physical Science, Aichi Gakuin University, Aichi, Japan

Long-term peritoneal dialysis induces peritoneal fibrosis with submesothelial fibrotic tissue. Although angiogenesis and inflammatory mediators are involved in peritoneal fibrosis, precise molecular mechanisms are undefined. To study this, we used microarray analysis and compared gene expression profiles of the peritoneum in control and chlorhexidine gluconate (CG)-induced peritoneal fibrosis mice. One of the 43 highly upregulated genes was pleiotrophin, a midkine family member, the expression of which was also upregulated by the solution used to treat mice by peritoneal dialysis. This growth factor was found in fibroblasts and mesothelial cells within the underlying submesothelial compact zones of mice, and in human peritoneal biopsy samples and peritoneal dialysate effluent. Recombinant pleiotrophin stimulated mitogenesis and migration of mouse mesothelial cells in culture. We found that in wild-type mice, CG treatment increased peritoneal permeability (measured by equilibration), increased mRNA expression of TGF-β1, connective tissue growth factor and fibronectin, TNF-α and IL-1β expression, and resulted in infiltration of CD3-positive T cells, and caused a high number of Ki-67-positive proliferating cells. All of these parameters were decreased in peritoneal tissues of CG-treated pleiotrophin-knockout mice. Thus, an upregulation of pleiotrophin appears to play a role in fibrosis and inflammation during peritoneal injury.

Kidney International (2012) **81,** 160–169; doi:10.1038/ki.2011.305; published online 31 August 2011

KEYWORDS: continuous ambulatory peritoneal dialysis; microarray analysis; peritoneal dialysis; peritoneal membrane

Correspondence: *Masato Kasahara, Department of Medicine and Clinical Science, Kyoto University Graduate School of Medicine, 54 Shogoin Kawahara-cho, Sakyo-ku, Kyoto 606-8507, Japan.*
E-mail: kasa@kuhp.kyoto-u.ac.jp

Received 8 December 2010; revised 19 June 2011; accepted 5 July 2011; published online 31 August 2011

Continuous ambulatory peritoneal dialysis (PD) is a preferred method of home dialysis for patients with end-stage renal failure.[1] Long-term use of PD induces peritoneal fibrosis characterized with the presence of submesothelial fibrotic tissue and increased peritoneal vascularization with vasculopathy.[2] Peritoneal fibrosis occurs in long-term continuous ambulatory PD patients in response to a variety of injuries, including bioincompatible dialysate solutions, peritonitis, uremia, and chronic inflammation.[2,3] Previous reports show that several profibrotic and proinflammatory mediators are upregulated upon induction of peritoneal fibrosis, such as transforming growth factor-β (TGF-β) and interleukin-6 (IL-6).[4–6] Although proinflammatory, angiogenic, and profibrotic cytokines such as IL-1β, vascular endothelial growth factor, and TGF-β are presumed to be involved in the pathogenesis, precise molecular mechanisms that lead to peritoneal sclerosis and encapsulating peritoneal sclerosis are still elusive.[7–9] To identify the novel genes possibly involved in the development of peritoneal fibrosis, we compared gene expression profiles of the peritoneum in chlorhexidine gluconate (CG)-induced peritoneal fibrosis and control mice using microarray.

Microarray analysis is a powerful tool to identify novel genes and pathways involved in the development of peritoneal fibrosis. Although a few papers report microarray analysis for endothelial cells in rat peritoneal dialysate infusion model,[10] analysis for whole mouse gene sets over 39,000 transcripts has not been investigated yet. In this study, we performed microarray analysis using a mouse model of peritoneal fibrosis and selected the genes that changed greatly in peritoneal fibrosis and those that were also present in mesothelial cells. This approach can allow us to specify the genes associated with peritoneal injury.

Here we show that one of the highly upregulated secreted proteins during the development of peritoneal fibrosis is pleiotrophin (PTN). PTN is an 18-kDa secreted protein, belonging to the midkine family and has functions similar to

midkine.[11] The receptors for PTN are the receptor protein tyrosine phosphatase β/ζ (RPTPβ/ζ), anaplastic lymphoma tyrosine kinase (ALK), and syndecan-3.[12] PTN has been shown to promote cell growth, migration, oncogenesis, and angiogenesis.[11] However, the role of PTN in peritoneal fibrosis remains unknown. To elucidate the role of PTN in peritoneal injury, we examined the PTN expression in a mouse model of peritoneal fibrosis and in human peritoneal biopsy samples. We also investigated the functional significance of PTN by using PTN-deficient mice.[13]

RESULTS

To screen novel genes involved in development of peritoneal fibrosis, we compared the gene expression profiles between phosphate buffered saline (PBS)-injected and CG-injected mice three times a week for 3 weeks. As a control, PBS-injected wild-type mice showed no peritoneal fibrosis. CG-injected mice showed marked thickened submesothelial peritoneal membrane compared with PBS-injected mice (Figure 1a, CG-injected mice: 228 μm vs. PBS-injected mice: 34 μm). We performed microarray analysis using parietal peritoneum in mice at 21 days after PBS and CG treatment. We identified genes differentially expressed between PBS- and CG-injected mice, which were also expressed in murine cultured mesothelial cells. Table 1 shows one downregulated and 43 upregulated genes that were expressed by eightfold or greater in CG-treated mice than that in PBS-treated wild-type mice, and which were expressed in the cultured mesothelial

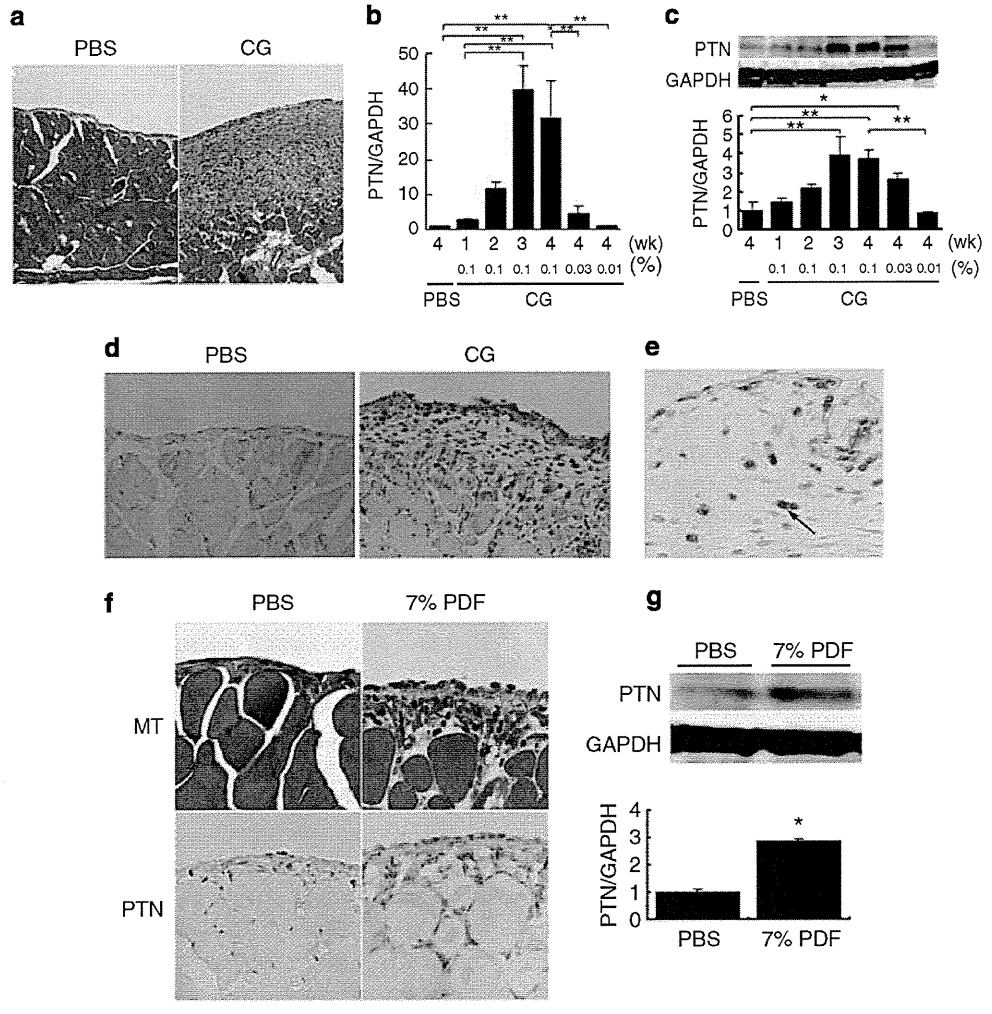

Figure 1 | PTN expression in a mouse model of peritoneal fibrosis. (**a**) Microscopic examination of peritoneal fibrosis model mice. C57BL/6J wild-type mice (WT) treated with phosphate-buffered saline (PBS) showed no fibrosis in the peritoneum. Chlorhexidine gluconate (CG)-treated mice exhibited marked peritoneal fibrosis with moderate infiltration of mononuclear cells on day 21 ($n=3$, each, original magnification × 20). Pleiotrophin (PTN) mRNA expression (**b**) or protein (**c**) in the peritoneum of PBS- or CG-treated mice was analyzed by real-time reverse transcriptase-polymerase chain reaction analysis or western blot analysis, respectively. GAPDH was used as internal control ($n=5$, each). (**d**) Immunohistochemical study for PTN (brown). Mesothelial cells and the cells in submesothelial layer were positive for PTN. (**e**) Double immunohistochemical study for PTN (brown) and S100A4 (blue). Some of PTN-positive cells were also positive for S100A4 (arrow). (**f**) Mice receiving daily intraperitoneal injection of 7% peritoneal dialysis fluid (PDF) for 4 weeks showed increased submesothelial layer thickness by Masson's trichrome staining (MT) and upregulated PTN protein in the submesothelial layer ($n=5$, each). (**g**) Western blot analysis showed that PTN protein in PDF-treated mice was 1.9 times higher than the control. GAPDH was used as internal control. Mean ± s.e. $^*P<0.05$, $^{**}P<0.01$ vs. PBS. GAPDH, glyceraldehyde-3-phosphate dehydrogenase; wk, week.

Table 1 | Genes changed in parietal peritoneum in chlorhexidine gluconate (CG)-treated mice compared with phosphate-buffered saline-treated mice after 3 weeks of CG treatment and in the presence of cultured mesothelial cells

Gene title	ID	Fold change of gene up- or downregulated in CG-treated mice compared with PBS-treated mice	Gene symbol
Glucocortoid-regulated inflammatory prostaglandin GH synthase (griPGHS)	M94967	168.897	*Ptgs2*
Procollagen, type VIII, alpha 1	NM_007739	73.51669	*Col8a1*
DEAD (Asp-Glu-Ala-Asp) box polypeptide 3, Y-linked	AA210261	55.71524	*Ddx3y*
Eukaryotic translation initiation factor 2, subunit 3, structural gene Y-linked	NM_012011	48.50293	*Eif2s3y*
A disintegrin and metallopeptidase domain 12 (meltrin alpha)	NM_007400	42.22425	*Adam12*
Interleukin 6	NM_031168	25.99208	*Il6*
Chemokine (C-X-C motif) ligand 1	NM_008176	24.25147	*Cxcl1*
Matrix metallopeptidase 14 (membrane-inserted)	NM_008608	24.25147	*Mmp14*
Chemokine (C-C motif) ligand 7	AF128193	17.14838	*Ccl7*
Ankyrin repeat domain 1 (cardiac muscle)	AK009959	16	*Ankrd1*
Leucine-rich repeat containing 15	AK017350	14.92853	*Lrrc15*
Chemokine (C-C motif) ligand 2	AF065933	14.92853	*Ccl2*
Interferon, alpha-inducible protein	AK019325	14.92853	*G1p2*
Runt-related transcription factor 1	NM_009821	12.12573	*Runx1*
Interferon regulatory factor 7	NM_016850	12.12573	*Irf7*
Collagen triple helix repeat containing 1	AK003674	12.12573	*Cthrc1*
Cytochrome P450, family 7, subfamily b, polypeptide 1	NM_007825	11.31371	*Cyp7b1*
Pleiotrophin	BC002064	11.31371	*Ptn*
Procollagen, type V, alpha 2	AV229424	11.31371	*Col5a2*
Fibronectin 1	BM234360	10.55606	*Fn1*
Chondroitin sulfate proteoglycan 2	NM_019389	10.55606	*Cspg2*
Thrombospondin 1	AI385532	10.55606	*Thbs1*
Membrane-spanning 4-domains, subfamily A, member 4C	NM_022429	10.55606	*Ms4a4c*
Lysyl oxidase	M65143	10.55606	*Lox*
Growth differentiation factor 15	NM_011819	9.849155	*Gdf15*
Dynamin 3, opposite strand	BB542096	9.849155	*Dnm3os*
RNA imprinted and accumulated in nucleus	BB649603	9.849155	*Rian*
WNT1-inducible signaling pathway protein 1	NM_018865	9.849155	*Wisp1*
Secreted frizzled-related sequence protein 1	BI658627	9.849155	*Sfrp1*
Procollagen, type III, alpha 1	AW550625	9.849155	*Col3a1*
Signal transducer and activator of transcription 2	AF088862	9.189587	*Stat2*
2′-5′ Oligoadenylate synthetase-like 2	BQ033138	9.189587	*Oasl2*
Tenascin C	NM_011607	9.189587	*Tnc*
Neural cell adhesion molecule 1	BB698413	8.574188	*Ncam1*
Integrin α5 (fibronectin receptor alpha)	BB493533	8.574188	*Itga5*
Tribbles homolog 3 (*Drosophila*)	BB508622	8.574188	*Trib3*
Gap junction membrane channel protein alpha 1	M63801	8.574188	*Gja1*
Interferon-induced protein with tetratricopeptide repeats 2	NM_008332	8.574188	*Ifit2*
Serine (or cysteine) peptidase inhibitor, clade A, member 3N	NM_009252	8.574188	*Serpina3n*
Lysyl oxidase-like 2	AF117951	8	*Loxl2*
GLI pathogenesis-related 2	BM208214	8	*Glipr2*
2′-5′ Oligoadenylate synthetase-like 1	AB067533	8	*Oasl1*
Tissue inhibitor of metalloproteinase 1	BC008107	8	*Timp1*
Immunoglobulin heavy chain 4 (serum IgG1)	BC008237	0.033493	*Igh4*

cells. Expression of extracellular matrix-related genes, including procollagen type VIII α1, was increased in peritoneal fibrosis model. Inflammatory cytokines including IL-6 were also upregulated. Among these upregulated genes, we focused on secreted proteins. One of them was PTN, which is an 18-kDa secreted protein and has been reported to promote mitogenesis and chemotaxis in cultured cells. Microarray analysis showed that PTN signal in the peritoneal membrane in the CG-injected wild-type mice was upregulated by 11-fold compared with PBS-injected mice (Table 1). Next, we confirmed the increase of PTN mRNA expression in the peritoneum of CG-treated mice by real-time reverse transcriptase-polymerase chain reaction (RT-PCR) analysis (Figure 1b). PTN mRNA in the peritoneum of CG-treated mice was gradually increased and peaked at 3 weeks by 39-fold compared with that in PBS-treated mice at 28 days, and was high until 4 weeks (Figure 1b). Diluted CG, such as 0.03 or 0.01%, induced weaker expression of PTN mRNA than 0.1% CG (Figure 1b). Western blot analysis also showed that PTN protein in the peritoneum of CG-treated mice was gradually upregulated and was highest at 3 weeks by 3.9-fold, as compared with that of PBS-treated mice (Figure 1c). A low concentration of 1:10 diluted CG induced less PTN expression (Figure 1c). Immunohistochemical study showed

that PTN was positive in the spindle-shaped cells and partly in mesothelial cells within the submesothelial layer (Figure 1d). Some of the spindle-shaped cells were also positive for a marker for fibroblasts S100A4, indicating that spindle-shaped cells were fibroblasts (Figure 1e). Next, we examined the effects of infusing peritoneal dialysis fluid (PDF) via a peritoneal catheter on expression of PTN. Mice receiving daily intraperitoneal injection of 7% PDF for 4 weeks showed increased PTN protein in the submesothelial layer with mild peritoneal fibrosis (Figure 1f). PTN protein in PDF-treated mice was 1.9 times higher than control mice, as observed by western blot analysis (Figure 1g).

We examined PTN expression in human biopsy samples at the insertion or removal of peritoneal catheters. PTN was expressed in human peritoneal biopsy samples by RT-PCR method (Figure 2a). Immunohistochemical study showed that PTN was located both in the mesothelial cells (arrows) and in the interstitial cells of peritoneal biopsy samples at the withdrawal from 5-year PD treatment (patient A), which was consistent with a mouse model of peritoneal fibrosis (Figure 2b). We examined whether peritoneal dialysate effluent contained PTN. Western blot analysis showed that peritoneal dialysates from six patients contained 15- and 18-kDa PTN (Figure 2c). The main form of PTN in peritoneal dialysate was 15 kDa. Patient B was a 54-year-old woman suffering from nephrosclerosis with a 2-year PD duration, patient C was a 47-year-old man suffering from diabetic nephropathy with a 2-year PD duration, and patient D was a 29-year-old woman suffering from immunoglobulin A nephropathy with a 1-year PD duration. Next, we examined PD effluent from patients with peritonitis. Patients E and F were 80- and 86-year-old women suffering from peritonitis by *Staphylococcus aureus*, respectively. PD effluents from patients with peritonitis tended to be high PTN levels. These results indicate that PTN exists in human peritoneal membrane and is detectable in peritoneal dialysate effluent.

Next, we investigated functional roles of PTN in cultured mouse peritoneal mesothelial cells. PTN exerts its effect, such as proliferation and chemotaxis, by binding its receptors, RPTPβ/ζ, ALK, and syndecan-3. We examined expression of Ptprz1, which encodes RPTPβ/ζ, ALK, and syndecan-3 in cultured mesothelial cells. Ptprz1 mRNA expression was detected in mesothelial cells but not in fibroblasts, macrophage cell line RAW264.7, mouse T-lymphoma cell line BW5147, mouse B-cell leukemia cell line BCL1-B20, or endothelial cell line bEnd.3 by real-time RT-PCR analyses (Figure 3a). Syndecan-3 mRNA expression was high in mesothelial cells and was also positive in fibroblasts, macrophages, and endothelial cells (Figure 3b). ALK mRNA expression was not detectable. PTN (1 ng/ml) stimulated proliferation in cultured mesothelial cells by 1.7-fold compared with vehicle-treated cells (Figure 3c). Angiotensin II and platelet-derived growth factor-BB stimulation showed less potent activity in cell proliferation than PTN, and endothelial growth factor treatment (100 ng/ml) revealed a similar potency to PTN stimulation (Figure 3c). PTN also induced mesothelial cell migration in the analysis of modified Boyden chamber method by threefold, as compared with vehicle-treated cells (Figure 3d). *In vitro*, fibroblasts cell line NIH3T3 fibroblasts showed higher PTN expression than mesothelial cells. RAW 264.7, mouse BW5147, BCL1-B20, and bEnd.3 showed virtually no expression of PTN (Figure 3e). These results indicate that PTN produced by fibroblasts may exert its biological effect on peritoneal mesothelial cells in the process of peritoneal fibrosis.

Finally, we examined whether PTN has a crucial role in peritoneal fibrosis progression. PTN knockout mice were treated with CG three times a week for 4 weeks. Although the thickness of peritoneal membrane in PTN knockout mice was similar compared with wild-type mice (Figure 4a and b), the expression of tumor necrosis factor-α and IL-1β mRNA was significantly reduced in CG-injected PTN knockout mice at 4 weeks, suggesting that PTN was involved in the inflammatory process (Figure 4c). Furthermore, gene expression of profibrotic factors, TGF-β1, connective tissue growth factor in CG-injected PTN knockout mice was reduced compared with CG-injected wild-type mice (Figure 4c). Fibronectin and type I collagen α1 chain were also decreased in CG-treated

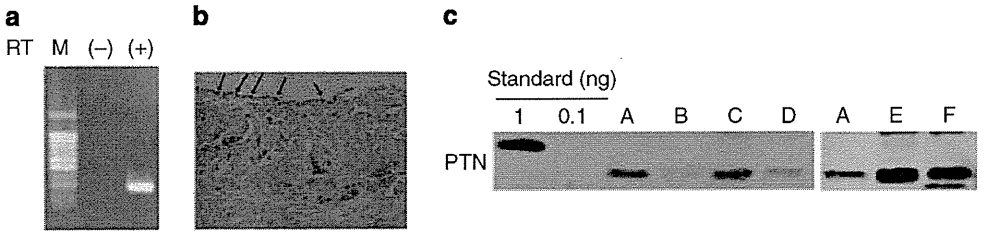

Figure 2 | PTN expression in human peritoneum and in peritoneal dialysate effluent. (**a**) Pleiotrophin (PTN) mRNA expression is detected by reverse transcriptase-polymerase chain reaction in human peritoneal biopsy sample. M, DNA marker (100 bp DNA ladder), RT (−) reverse transcriptase (−), RT (+) reverse transcriptase (+). (**b**) Immunohistochemical study for PTN in the peritoneal biopsy sample from a 5-year peritoneal dialysis (PD) patient A. (**c**) Western blot analysis for PTN in peritoneal dialysate effluent. Patient B was a 54-year-old woman suffering from nephrosclerosis with a 2-year PD duration, patient C was a 47-year-old man suffering from diabetic nephropathy with a 2-year PD duration, and patient D was a 29-year-old woman suffering from immunoglobulin A nephropathy with a 1-year PD duration. Patients E and F suffered from peritonitis by *Staphylococcus aureus*, and their PD efferents were shown on the first day of the peritonitis. Patient E was an 80-year-old woman suffering from nephrosclerosis with a 3-year PD duration. Patient F was an 86-year-old woman suffering from diabetic nephropathy with a 4-year PD duration.

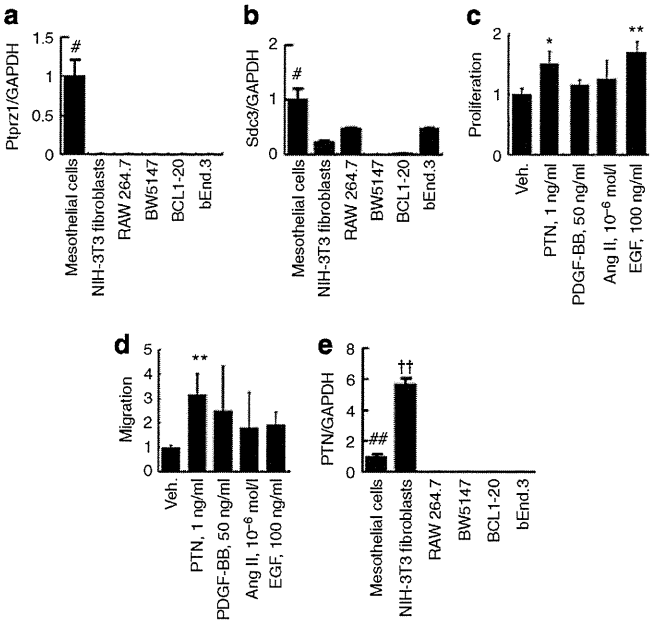

Figure 3 | PTN, Ptprz1, and syndecan-3 expression in cultured cells. The effect of pleiotrophin (PTN) on cell proliferation and migration in cultured mesothelial cells. (**a**) Ptprz1 mRNA expression was quantified by real-time reverse transcriptase-polymerase chain reaction (RT-PCR) in cultured mesothelial cells, NIH3T3 fibroblasts, RAW264.7, BW5147, BCL1-20, and bEnd.3 cells ($n=6$, each). (**b**) Syndecan-3 (Sdc3) mRNA expression was quantified by real-time RT-PCR in cultured mesothelial cells, NIH3T3 fibroblasts, RAW264.7, BW5147, BCL1-20, and bEnd.3 cells ($n=6$, each). (**c**) The effect of PTN on cell proliferation in cultured mesothelial cells. Mesothelial cells were treated with PTN (1 ng/ml), platelet-derived growth factor (PDGF)-BB (50 ng/ml), angiotensin II (Ang II, 10^{-6} mol/l), endothelial growth factor (EGF, 100 ng/ml), or vehicle (Veh.). ^{3}H-thymidine incorporation was assessed ($n=6$, each). (**d**) The effect of PTN on cell migration in cultured mesothelial cells by modified Boyden chamber method. Mesothelial cells were treated with PTN (1 ng/ml), PDGF-BB (50 ng/ml), angiotensin II (10^{-6} mol/l), or EGF (100 ng/ml) ($n=6$, each). (**e**) PTN mRNA expression was quantified by real-time RT-PCR in cultured mesothelial cells, NIH3T3 fibroblasts, RAW264.7, BW5147, BCL1-20, and bEnd.3 cells ($n=6$, each). Mean ± s.e. $^{*}P<0.05$, $^{**}P<0.01$ vs. vehicle. $^{\#}P<0.05$, $^{\#\#}P<0.01$ vs. NIH3T3 fibroblasts, BW264.7, BW5147, BCL1-20 or bEnd.3. $^{\dagger\dagger}P<0.01$ vs. mesothelial cells, RAW264.7, BW5147, BCL1-20 or bEnd.3. GAPDH, glyceraldehyde-3-phosphate dehydrogenase.

PTN knockout mice. On the other hand, expression of type IV collagen α1 chain was increased with the CG injection and was similar between wild-type and PTN knockout mice with CG treatment (Figure 4c). Macrophage infiltration was assessed by immunohistochemical study for F4/80. The number of macrophages in the peritoneum was increased in CG-injected wild-type mice. The number tended to decrease, but not significantly altered in CG-injected PTN knockout mice at 4 weeks (Figure 5a–d and q). In contrast, the number of CD3-positive T cells per the number of total cells in submesothelial area in CG-treated PTN knockout mice was significantly reduced compared with that in CG-treated wild-type mice at 4 weeks (5.6 ± 0.9 vs. 10.3 ± 0.5; Figure 5e–h and r). The effect of PTN on cell proliferation was evaluated by immunohistochemical study for Ki-67, a marker for cell proliferation (Figure 5i–l and s). Interestingly, immunohistochemical study showed that Ki-67-positive cells were localized within submesothelial compact zone and that cells positive for Ki-67 were presumed to be fibroblast-like cells according to their morphological appearance in CG-treated wild-type mice. The number of Ki-67-positive cells in CG-treated PTN-deficient mice was significantly decreased compared with that in CG-treated wild-type mice (1.5 ± 1.1 vs. 3.8 ± 1.2). Collagen IV deposition was similar between CG-treated wild-type mice and CG-treated PTN-deficient mice (Figure 5m–p). Peritoneal equilibration test was conducted to examine the functional role of PTN on peritoneal fibrosis at 2 weeks after the first CG injection. Figure 6 showed that the ratio of creatinine concentrations in the dialysate multiplied by dialysate volume over the plasma creatinine (D Cr × volume/P Cr) in PBS-treated PTN-deficient mice was not different from that in PBS-treated wild-type mice. In contrast, D Cr × volume/P Cr in CG-treated PTN-deficient mice was lower than that in CG-treated wild-type mice (1.93 ± 0.15 vs. 2.33 ± 0.38), suggesting that PTN deficiency was associated with low peritoneal transport in peritoneal fibrosis.

These results suggest that PTN has a crucial role in cell proliferation, extracellular matrix production, and peritoneal permeability during the development of peritoneal fibrosis through inflammatory process.

DISCUSSION

In this study, we identify for the first time that PTN is expressed in peritoneal tissues in mice and humans, especially in experimental peritoneal fibrosis mouse model. Mice receiving intraperitoneal infusion of PDF also showed increased expression of PTN, suggesting that PTN could be involved in peritoneal injury induced by dialysis solution. PTN is an 18- or 15-kDa heparin-binding protein.[11,14] PTN is initially identified as a neurite growth/guidance-regulating protein and belongs to the midkine family.[15,16] PTN has diverse functions including proliferation, mitogenic activities, apoptosis, oncogenic activity, and angiogenic activity.[11] PTN has been shown to have an important role in embryogenesis and kidney development.[17] PTN-deficient mice have been shown to have lower threshold for induction of long-term potentiation in hippocampal slices.[18] Other reports show that PTN-deficient mice exhibit less migration of neutrophils and macrophages to liver after partial hepatectomy,[19] and that female mice deficient in both midkine and PTN are infertile.[13]

The long-term PD can cause deterioration of the peritoneum,[20] and is closely associated with high peritoneal transport rate, which is one of the risk factors for developing encapsulating peritoneal sclerosis.[21] To evaluate the degree of peritoneal damage, several biomarkers have been investigated. Dialysate concentrations of IL-6 and vascular endothelial growth factor have been shown to be associated with increased peritoneal transport rate.[4] Dialysate fibrinogen/